Utrecht University

Institute of Theoretical Physics

Master Thesis

The magnon-drag Peltier effect

Author:
H.A.Q. Enneking

Supervisors:
Prof. Dr. R.A. Duine
Dr. S.A. Bender

Abstract

In this thesis we set out to find signatures of magnonic black hole horizons in transport experiments. Using the stochastic Landau-Lifshitz-Gilbert equation, we perform calculation of the magnon-drag Peltier coefficient in the axial configuration that agrees with the result from B. Flebus *et al.* [11]. We generalize the calculation to the easy-plane configuration. Finally, we discovered a threshold value for the magnon drift velocity, which corresponds to the transition between a super- and subsonic regime for the magnons and show that the supersonic regime can be unstable.

June 30, 2017

Contents

1 Introduction

Magnons are quasiparticles, meaning they do not consist of ordinary matter, but instead correspond to collective excitations, in this case, in the magnetization. They were first introduced by Felix Bloch [1] in order to better understand the appearance of ordered spin states in ferromagnets at zero applied magnetic field and zero temperature. At absolute zero temperature, a system of atomic particles in a ferromagnet has its spin completely aligned to maximize the net magnetization and minimize the exchange interactions. When the temperature is increased, spins start to deviate randomly from the common direction defined by the ground state of the system. If one were to treat the perfectly magnetized state at $T = 0$ as the vacuum state of the system, the $T \neq 0$ state with increased internal energy and decreased net magnetization can be treated as a gas of quasiparticles, i.e. magnons. According to the laws of quantum mechanics, the change of a single particle's spin angle is equal to the partial shift of the spin angles of all particles in the system. This partial disturbance then travels through the lattice like a wave of discrete energy transferal. We may call this wave a spin wave, because the magnetization is induced by the spins of the particles. This concept is illustrated in Fig.1 below, where is shown how the spins align with the magnetic field after a strong pulse and induce changes in orientation of the surrounding spins, effectively creating a spin wave. Thus we conclude that magnons are in fact quantized spin waves.[1]

In the early 70's, Hawking suggested that black holes evaporate via a quantum instability by radiating particles with a thermal spectrum [18], thus combining quantum mechanics and gravity to produce thermodynamics. However, Hawking radiation from gravitational black holes has never been measured. As Unruh [17] suggested however, the observation of this radiation can be quite challenging due to a number of reasons. In part, this is due to the Hawking temperatures of astronomical black holes being too low to observe. As it seems highly unlikely that we discover a small (i.e. primordial) black hole in the vicinity of the Earth, other methods should

[1] This part has been taken directly from my Bachelor thesis [2].

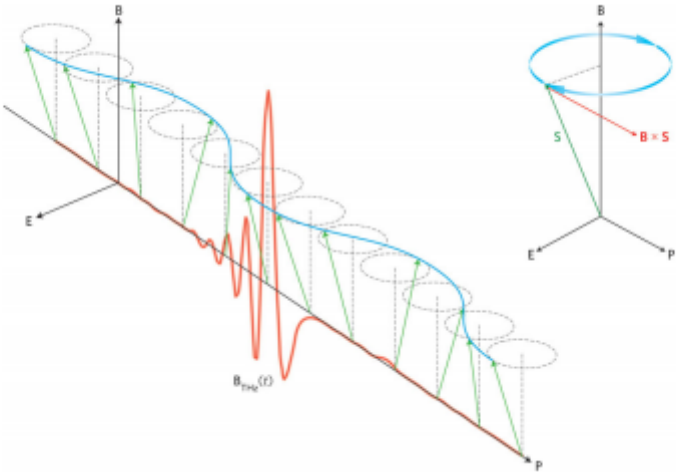

Figure 1: Magnon propagation after an ultrashort terahertz magnetic field pulse (red)- the magnon is shown by the blue line connecting the spin tips. Taken directly from [16]

be considered. Creating smaller black holes - which should have higher Hawking temperatures - seems experimentally impossible. Another reason is that, even if one would succeed, they would still evaporate rapidly. To bypass the complications outlined above and to improve upon the theoretical treatment of Hawking radiation, Unruh proposed the experimental creation of black hole horizon analogues. The model he describes is one of the motion of sound in a convergent fluid. A black hole horizon for sound waves in a flowing medium is created by a transition from the subsonic to supersonic regime, such that waves along the flow and incoming from the subsonic region cannot escape from the supersonic region. A white hole horizon is then a region where the flow goes from the supersonic to subsonic regime. In that case, a wave travelling against the flow from the subsonic region cannot penetrate the supersonic part. Essential to the formation of analogue horizons is that the background velocity can exceed the wave velocity and that the waves are linearly dispersing at long wavelengths. [10, 17].

In this thesis, we consider a black hole analogue in a solid-state system, as proposed in [10]. In particular, a ferromagnetic system subjected to a charge current, in which the flowing electron spins can become partially spin-polarized. These electrons can then affect the magnetization dynamics, which is known as spin-transfer torque [19]. These spin-transfer torques constitute the interaction between a spin-polarized electric current through a magnetic conductor and the magnetization dynamics. This gives the spin-waves, or magnons, a Doppler-shift with effective spin-drift velocity $\vec{v_s}$. The previously discussed supersonic and subsonic regimes then translate into regions where (the absolute value of) the drift velocity $\vec{v_s}$ is respectively larger or smaller than the spin-wave velocity c [10].

The question that rises is: how can we measure the presence of a magnonic black hole horizon? Here we consider signatures in transport measurements and we closely follow the paper by B. Flebus *et al.* [11], where the Seebeck coefficient, or magnon-drag thermopower, is calculated from the stochastic Landau-Lifshitz-Gilbert (LLG) equation. Here the system is subjected to a temperature gradient and exhibits a magnonic drag of the electric current. The long-wavelength magnetic dynamics result in two contributions to the electromotive force acting on electrons, the first being an adiabatic Berry-phase force moving electrons to the hot side and the second being a dissipative correction of this Berry-phase force, moving the electrons towards the cold side, i.e. in the direction of magnonic drift. In our case, we set out to calculate the reciprocal of the Seebeck effect, namely the (magnon-drag) Peltier effect. An added benefit is that we can check whether Onsager's reciprocity, to be outlined later on, holds in the thermoelectric case, for the (magnon-drag) Seebeck and Peltier effects. The main goal of this thesis is to develop a theory to observe signatures of magnonic black holes in the Peltier coefficient.

Below we first expand on the transport phenomenology underlying the theory we set out to develop. This chapter is subdivided into multiple paragraphs where we describe the fundamental concepts involved with transport. We further outline the concepts of Peltier and Seebeck effects, introduce the magnon-drag effect and Onsager's reciprocity and explain how the spin transfer torques contribute to the magnon-drag and to the creation of magnonic black hole horizon. In section 3, we outline the calculations and also discuss the corresponding results. We calculate the Peltier effect for two different models, one being the simple axial configuration with no anisotropy and the other one being the easy-plane configuration. We also discuss the dynamic (in)stability of the models for different values of $\vec{v_s}$. Finally, we draw our conclusions based on the results in this thesis and present the reader with an outlook on future developments.

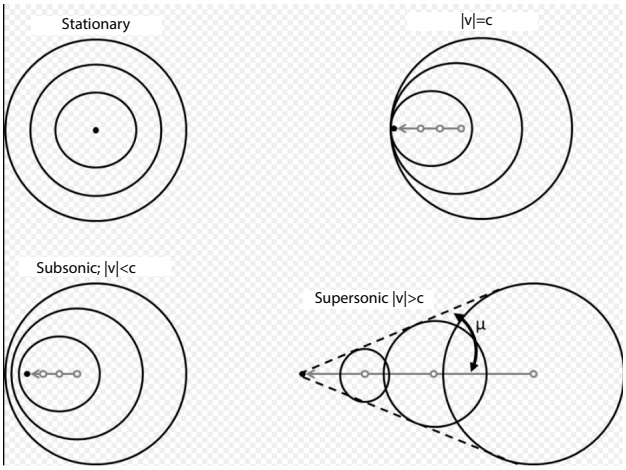

Figure 2: Depiction of the different regimes for the magnon cloud with respect to the background current velocity. As $\vec{v}_s$ becomes greater than c, the transition to the supersonic regime is associated with a sonic boom. Image taken from the internet.

2 Transport phenomenology

In this section we elaborate on the phenomenology of some key concepts underlying the theory of magnetism and transport. In particular, these concepts are spin transport and its associated thermoelectric effects, the occurrence of magnon-drag and finally Onsager's reciprocity, which tells us how certain effects are related to one another. Thermoelectric effects may be viewed as the mutual interference of heat and electric current flow within a system.

2.1 Spin transport

The fields of research on spintronics and spin caloritronics focus primarily on understanding interactions between spin dynamics and transport phenomena in ferromagnetic metals. Of particular interest are the thermal properties of spin dynamics, or magnon scattering mechanisms, at finite temperature [3]. Spintronics, an abbreviation for spin transport electronics, differs from regular electronics in the sense that it offers an additional degree of freedom. Indeed, spintronics exploits the intrinsic spin of an electron and its corresponding magnetic moment, which has implications in the efficiency of data transfer and storage. Spin caloritronics is a relatively new field of research and focuses specifically on the interaction of spins with heat currents, motivated by the continuing discovery of new thermoelectric effects. Two of the most fundamental thermoelectric phenomena are the Seebeck and Peltier effects. These effects couple heat, charge and spin in magnetic materials. The Seebeck effect describes the direct conversion of a thermal gradient to an electric voltage. Conversely, the Peltier effect is a temperature difference developed across a material in response to an applied voltage. At the atomic scale, this corresponds to an applied temperature gradient causing charge carriers to move from the hot to the cold side of the material, inducing a measurable voltage. The Peltier effect can be viewed as the back-action counterpart to the Seebeck effect, analogous to the back-emf in magnetic induction. The Peltier and Seebeck effects are thermodynamically reversible, a fact we will use later on when deriving the Onsager reciprocal relations [4].
Before we can discuss the effects of magnon-electron coupling, we must first revisit the phe-

nomenology concerning magnons and electrons separately. One can apply a temperature gradient on electrons, inducing three different effects. One effect is when the electrons heat up, causing charge to be transported along the system inducing an electron charge current. This charge current constitutes the (regular) Seebeck effect, converting the temperature gradient into a voltage. The moving electrons also cause an electron spin current, which is associated with the recently discovered spin-dependent Seebeck effect [20, 21]. Naturally, a temperature gradient also causes an electron heat current to flow through the system. If we consider inducing a voltage rather than a temperature gradient, we can identify the three reciprocal effects: electron charge current (electricity), the electron spin current associated with a spin-polarized current and finally the electron heat current constituting the (regular) Peltier effect. This summarizes regular electronics; we proceed in a similar fashion in the case of magnons. Since magnons do not have charge, it is meaningless to consider the effect of an applied voltage. However, a temperature gradient applied to magnons specifically causes a magnon spin current (spin-Seebeck [22]) as well as a magnon heat current. If we switch on magnon-electron coupling, we can understand the process of [11] a lot better: B. Flebus *et al.* start with a magnonic temperature gradient, which induces a magnon spin current. This magnon spin current then gives rise, through magnon-electron coupling, to an electron spin, charge and heat current. They focus on the resulting charge current and determine the corresponding Seebeck coefficient, also known as the magnon-drag thermopower. The underlying mechanism of magnon-electron coupling is constituted by spin-transfer torques and describes the process of electron spins interacting with the magnon spins. Effectively, this interaction gives the magnon cloud a nonzero drift velocity by dragging the magnons along. This is known as magnon-drag and will be discussed further in the next section. Finally, we are able to describe the main goal of this thesis in more detail. We apply a voltage to our ferromagnet, resulting in an electron spin current flow and thus a spin-polarized current. Through the same spin torque coupling as described above, a magnon current is established. This magnon current consists of a magnonic spin and a magnonic heat contribution to the current. The magnon heat current is our main topic of interest in this thesis and its Peltier analogue is named, due to its origin in the magnon-electron coupling, the magnon-drag Peltier effect. In summary, the application of a voltage to our system creates an electron heat current and a magnon heat current. The former causes the (regular) Peltier effect and the latter is what constitutes the magnon-drag Peltier effect. Here we set out to specifically calculate the magnonic contribution to the total Peltier effect, such that we can compare our results with [11]. The reciprocal magnon-drag Peltier and Seebeck effects, and therefore the main setup of this thesis, are depicted in Fig. 3. Finally, to further illustrate the difference between the regular and spin Seebeck effect, we have included Fig 4.

2.2 Magnon-drag

Contrary to spin-dependent thermoelectric effects carried by electron spin-up and spin-down currents, only magnons can drive the spin Seebeck and Peltier effects [5]. The magnon-drag effect is the result of collisions between the magnons and electrons in an insulating ferromagnet. Because of this, the electric current causes the magnon gas to have a non-equilibrium distribution resulting in an average drift velocity $\vec{v_s}$ and a corresponding nonzero heat current. The way this works is that the spin torques transfer angular momentum and energy from the electrons to the magnons, by means of collision, thereby cooling the electrons and heating the magnons, effectively inducing a magnon temperature gradient. This drag effect is very similar to phonon-drag, where the effective mass of conducting electrons increases as they interact with the crystal lattice in which the electrons move. In general, magnon-drag is more important at higher temperatures (though T is still below the Curie temperature T_c), while phonon-drag becomes

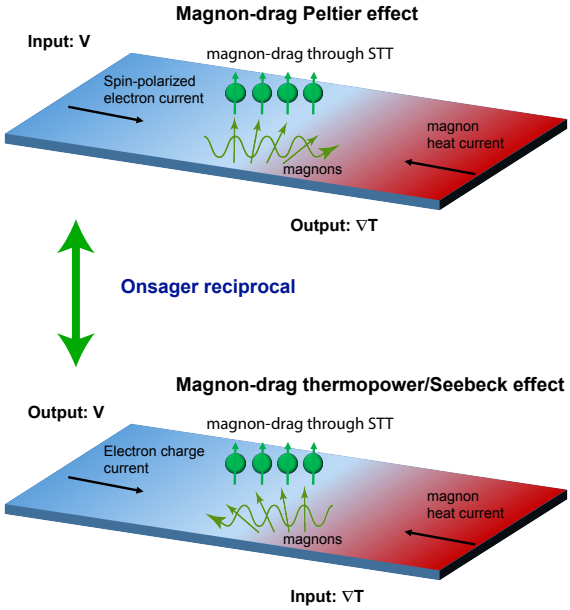

Figure 3: This figure shows the relation between the magnon-drag Seebeck and Peltier effects. Above, an induced voltage gives rise to an electron spin current. Through spin-transfer torques, a magnon current arises consisting of a spin and heat current. The heat current constitutes the magnon-drag Peltier effect. Below, a temperature gradient applied to magnons induces, through coupling, a electron current which consists of a spin, charge and heat contribution. The charge current gives rise to the magnon-drag thermopower.

the dominant contribution at lower temperatures [6]. What this means for the spin Seebeck effect is the following: a temperature gradient maintained in a system will drive phonon and electron transport. If the system does not allow for a steady-state current to run (i.e. open-circuit condition), the charge flows until the electric field balances the heat flow through the system. The resulting voltage drop is what constitutes the Seebeck coefficient, which follows from $S = \Delta V/\Delta T$. The Seebeck coefficient is sometimes also referred to as the thermopower of a systm. Spin-waves, or magnons, in magnetic films can increase ΔV by transporting additional energy from the phonons to the electrons. The increase in S through magnons is what is known as magnon-drag [3]. The magnon-drag phenomenon contributes analogously to the Peltier effect by magnon-electron coupling.

2.3 Onsager's reciprocity

Onsager's reciprocity [8] is the main result in the thermodynamics of non-linear processes. In order to be able to apply Onsager's reciprocity to steady-state processes of the thermoelectric kind, we use the notion of local equilibrium. The reciprocity is a very general statement and assumes microscopic reversibility applied to fluctuations. This can be interpreted as the requirement

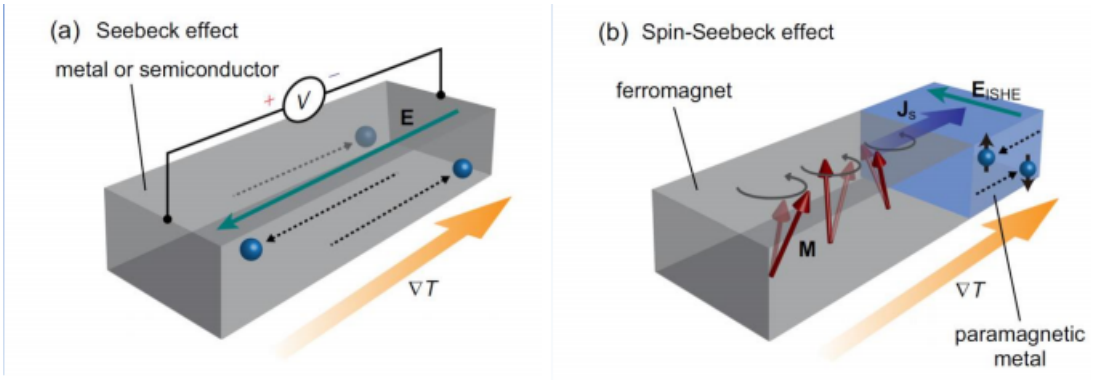

Figure 4: In a), the regular Seebeck effect is depicted which converts a voltage into a temperature gradient. Magnons play no part in this effect. In b), however, the magnons transfer the energy and angular momentum to electrons, resulting in a charge potential or voltage. This image was taken directly from [24].

that the processes be thermodynamically reversible. It also relates generalized thermodynamical forces to generalized currents. The derivation of the reciprocal relations follows from considering the generalized mathematical expression:

$$\dot{q}_i = \sum_{j-1}^{N} L_{ij} X_j, \tag{1}$$

where $\dot{q}_i$ is a generalized current, X_j is a generalized force and L_{ij} is the coefficient which relates the two. Onsager's reciprocity states that the off-diagonal elements of the matrix L should be equal to each other, i.e. $L_{ij} = L_{ji}$, due to the time reversibility of microscopic dynamics. This implies that the relations hold if the system maintains time-reversal symmetry [4]. Onsager's contribution was that he showed that not only L is a positive definite matrix, but also that it is symmetric under time reversibility. If we now apply the conditions above to our system, we can write the Onsager reciprocal relations as a linear response matrix. The linear response matrix of thermoelectrics reflects the Onsager's reciprocity when the sum of the products of currents and driving forces equals the dissipation [5]. Therefore, let us define the charge current $\vec{j_C}$ and heat current $\vec{j_Q}$. Since the spin Seebeck effect generates a charge current and the spin Peltier effect generates a heat current, we can denote the relation in a linear response matrix for thermoelectric effects. Note that the total Seebeck and Peltier effects are composed of two contributions, but we consider only the magnonic parts. We denote these by S_m and Π_m respectively. The linear response matrix then looks like:

$$\begin{pmatrix} j_C \\ j_Q \end{pmatrix} = \begin{pmatrix} \sigma & \sigma S_m T \\ \sigma \Pi_m & \kappa \end{pmatrix} \begin{pmatrix} E \\ -\frac{\nabla T}{T} \end{pmatrix}. \tag{2}$$

Here σ is the electrical conductance, κ represents the heat conductivity of the system and E is the electric field corresponding to a voltage difference. The off-diagonal elements are the magnon-drag Seebeck coefficient S_m and magnon-drag Peltier coefficient Π_m; Onsager's reciprocity therefore predicts that they should satisfy: $\Pi_m = TS_m$. Now that we have reviewed the key concepts at hand, we are ready to move on to the calculation of the magnon-drag Peltier coefficient in the next part. We start with the axial configuration to verify reciprocal agreement of the magnon-drag thermopower in [11].

3 Calculation of the magnon-drag Peltier coefficient

We begin our calculations by looking at a general expression for the LLG equation, taken from [12], rewritten in dimensions of energy:

$$\hbar\frac{\partial\vec{n}}{\partial t} = \vec{n}\times\left(-\frac{\delta E[\vec{n}]}{\delta\vec{n}}\right) - \hbar\alpha\vec{n}\times\frac{\partial\vec{n}}{\partial t} + \hbar\frac{\partial\vec{n}}{\partial t}\bigg|_{STT}. \tag{3}$$

Here $\vec{n} = \vec{n}(\vec{r},t)$ is the directional order parameter or magnetization vector. This magnetization vector is normalized to unit magnitude and the self-consistent spin density is given by $\vec{s} = s\vec{n}$. Moreover, the terms proportional to α and β represent the damping terms and will be discussed in more detail when we define the stochastic LLG equation. The first term on the right hand side describes the precession of the magnetization around an effective field, written here as an functional derivative of the magnetic energy. For smooth spin-textures, the spin-transfer torque (STT) terms can be expressed as [12]:

$$\frac{\partial\vec{n}}{\partial t}\bigg|_{STT} = -\left(\vec{v}_s\cdot\vec{\nabla}\right)\vec{n} - \beta\vec{n}\times\left(\vec{v}_s\cdot\vec{\nabla}\right)\vec{n}, \tag{4}$$

The magnetic energy functional contains contributions from the Zeeman coupling of the magnetization to the external magnetic field B, anisotropy energy contributions due to spin-orbit coupling and magnetostatic interactions and the energy cost of magnetization variation, which is proportional to the exchange stiffness A. In the case of an applied magnetic field B and anisotropy K in the z-direction, we retrieve the relatively simple model of the easy-plane ferromagnet. The anisotropy induces a tilt towards to xy-plane. In this case, the easy-plane Hamiltonian is of the form:

$$\mathcal{H} = \int d^3r\left(-\frac{A}{2}\vec{n}\cdot\nabla^2\vec{n} + Bs_z + \frac{1}{2s}Ks_z^2\right). \tag{5}$$

We are interested in calculating the functional derivative of Eq. 5, such that we can obtain the effective field in the LLG equation. We start by considering the following expression for the magnetic energy functional:

$$E[\vec{n}] = \int d^3r\ \left(-\frac{A}{2}\vec{n}\cdot\nabla^2\vec{n} + s\vec{B}\cdot\vec{n} + \frac{s}{2}n_z^2K\right) \equiv \int d^3r\ \varepsilon_m. \tag{6}$$

Since we can express our energy functional as an integral of a function and its derivatives, we apply the general formula

$$\frac{\delta F}{\delta\rho(\vec{r})} = \frac{\partial f}{\partial\rho} - \vec{\nabla}\cdot\frac{\partial f}{\partial\nabla\rho}, \quad \text{for a functional} \quad F[\rho] = \int d^3r\ f(\vec{r},\rho(\vec{r}),\nabla\rho(\vec{r})). \tag{7}$$

First, we integrate the first term by parts in our energy functional. This allows us to easily calculate the derivatives in Eq.7 and it is therefore straightforward to show that

$$\begin{aligned}\frac{\delta E[\vec{n}]}{\delta\vec{n}} &= \frac{1}{s}\left(\frac{\partial\varepsilon_m}{\partial\vec{n}} - \vec{\nabla}\cdot\frac{\partial\varepsilon_m}{\partial\vec{\nabla}\vec{n}}\right)\\ &= B\hat{z} + n_zK\hat{z} + \vec{h} - \frac{A}{s}\vec{\nabla}\cdot(\vec{\nabla}\vec{n})\\ &= B\hat{z} + n_zK\hat{z} + \vec{h} - \frac{A}{s}\nabla^2\vec{n},\end{aligned} \tag{8}$$

Note that, to account for dimensional consistency, a factor of $1/s$ was included since ε_m has dimensions of energy density; JL^{-3}. We now wish to find the corresponding current $\vec{j}_{\varepsilon,m}$ obeying the relation $\partial_t \varepsilon_m = -\vec{\nabla} \cdot \vec{j}_{\varepsilon,m}$. Since the current is a conserved quantity, the damping and stochastic terms can not be taken into consideration as these do not, by definition, conserve energy. Therefore we set $\alpha = \beta = \vec{h} = \vec{v}_s = 0$ for the duration of this calculation. Our equation of motion follows from Eq. 3 and under said restrictions, reduces to:

$$\hbar \partial_t \vec{n} = -\vec{n} \times \left(B\hat{z} + n_z K \hat{z} - \frac{A}{s} \nabla^2 \vec{n} \right). \tag{9}$$

We take the time derivative of ε_m in absence of anisotropy, because the terms proportional to it will vanish later on when we perform the linearization. The time derivative becomes:

$$\partial_t \varepsilon_m = -\frac{A}{2} \partial_t \vec{n} \cdot \nabla^2 \vec{n} + s\vec{B} \cdot \partial_t \vec{n} - \frac{A}{2} \vec{n} \cdot \nabla^2 \partial_t \vec{n}. \tag{10}$$

Plugging in our equation of motion, for $K = 0$, into Eq.10 and using the fact that the cross product of a vector with itself is always zero, we obtain

$$\begin{aligned} \hbar \partial_t \varepsilon_m = &\frac{A}{2} \left(\vec{n} \times \left(\vec{B} - \frac{A}{s} \nabla^2 \vec{n} \right) \right) \cdot \nabla^2 \vec{n} - s\vec{B} \cdot \left(\vec{n} \times \left(\vec{B} - \frac{A}{s} \nabla^2 \vec{n} \right) \right) \\ &+ \frac{A}{2} \vec{n} \cdot \left(\nabla^2 \vec{n} \times \vec{B} - \frac{A}{s} \vec{n} \times \nabla^4 \vec{n} \right). \end{aligned} \tag{11}$$

The scalar triple product rule for general vectors $\vec{a}$, $\vec{b}$ and $\vec{c}$ tells us that the product remains unchanged if we cyclically permute the three vectors. Furthermore, we have that if any of the three vectors are equal to each other, the scalar triple product will reduce to zero as it can be permuted such that a cross product between two equal vectors is obtained, which is zero. Therefore, we are left with

$$\begin{aligned} \hbar\, \partial_t \varepsilon_m &= \frac{A}{2} \left(\vec{n} \times \vec{B} \right) \cdot \nabla^2 \vec{n} + A \left(\vec{n} \times \nabla^2 \vec{n} \right) \cdot \vec{B} + \frac{A}{2} \left(\nabla^2 \vec{n} \times \vec{B} \right) \cdot \vec{n} \\ &= \frac{A}{2} \left(\vec{n} \times \vec{B} \right) \cdot \nabla^2 \vec{n} - A \left(\vec{n} \times \vec{B} \right) \cdot \nabla^2 \vec{n} - \frac{A}{2} \left(\vec{n} \times \vec{B} \right) \cdot \nabla^2 \vec{n} \\ &= -A \left(\vec{n} \times \vec{B} \right) \cdot \nabla^2 \vec{n}. \end{aligned} \tag{12}$$

Since we want to retrieve an expression for the current, we recall that this is defined as $\partial_t \varepsilon_m = -\vec{\nabla} \cdot \vec{j}_{\varepsilon,m}$. Suppose we define our current as $\vec{j}_{\varepsilon,m} = \frac{A}{\hbar} \left(\vec{\nabla} \vec{n} \times \vec{n} \right) \cdot \vec{B}$, then taking the divergence of this quantity gives us

$$\begin{aligned} -\vec{\nabla} \cdot \vec{j}_{\varepsilon,m} &= -\vec{\nabla} \cdot \left(\frac{A}{\hbar} \left(\vec{\nabla} \vec{n} \times \vec{n} \right) \cdot \vec{B} \right) \\ &= -\frac{A}{\hbar} \left(\left(\nabla^2 \vec{n} \times \vec{n} \right) \cdot \vec{B} + \left(\vec{\nabla} \vec{n} \times \vec{\nabla} \vec{n} \right) \cdot \vec{B} + \left(\vec{\nabla} \vec{n} \times \vec{n} \right) \cdot \vec{\nabla} \vec{B} \right) \\ &= -\frac{A}{\hbar} \left(\nabla^2 \vec{n} \times \vec{n} \right) \cdot \vec{B} \\ &= -\frac{A}{\hbar} \left(\vec{n} \times \vec{B} \right) \cdot \nabla^2 \vec{n}. \end{aligned} \tag{13}$$

Comparing the above with Eq.12, we see that our definition of the current is indeed correct as it yields the required result. Now that we have found an expression for the current, we want to

write it solely in terms of the order parameter. Therefore, we return to the restricted equation of motion Eq.9 in order to express $\vec{B}$ in terms of $\vec{n}$. We have that

$$\vec{n} \times \vec{B} = A\vec{n} \times \nabla^2 \vec{n} - \hbar\, \partial_t \vec{n}. \tag{14}$$

Looking at this expression, we try a solution of the form $\vec{B} = \hbar\, \vec{n} \times \partial_t \vec{n} + \frac{A}{s} \nabla^2 \vec{n}$:

$$\begin{aligned} \vec{n} \times \vec{B} &= \vec{n} \times (\hbar \vec{n} \times \partial_t \vec{n}) + \frac{A}{s} \vec{n} \times \nabla^2 \vec{n} \\ &= \hbar\, (\vec{n} \cdot \partial_t \vec{n})\, \vec{n} - \hbar\, |\vec{n}|^2 \partial_t \vec{n} + \frac{A}{s} \vec{n} \times \nabla^2 \vec{n} \\ &= \frac{A}{s} \vec{n} \times \nabla^2 \vec{n} - \hbar\, \partial_t \vec{n}, \end{aligned} \tag{15}$$

where we used the fact that $\vec{n}$ is a unit vector such that $|\vec{n}|^2 = 1$ and $\vec{n} \cdot \partial_t \vec{n} = 0$. Indeed, this returns Eq. 14 as desired, therefore we plug the expression for $\vec{B}$ into the current:

$$\begin{aligned} \vec{j}_{\varepsilon,m} &= A(\vec{\nabla} \vec{n} \times \vec{n}) \cdot (\vec{n} \times \partial_t \vec{n}) + \frac{A^2}{\hbar s} (\vec{\nabla} \vec{n} \times \vec{n}) \cdot \nabla^2 \vec{n} \\ &= A(\vec{\nabla} \vec{n} \times \vec{n}) \cdot (\vec{n} \times \partial_t \vec{n}) + \mathcal{O}\left(\nabla^3 \vec{n}\right), \end{aligned} \tag{16}$$

where we neglected terms with higher than second order derivatives. This expression for the heat current is as far as we can go at the moment. Later on, we linearize around the z-axis, allowing us to reduce the expression further.

All of the above finally allows us to define the LLG equation as we will use it throughout this thesis. Writing out Eq. 3 and rearranging some of the terms results in the following LLG equation, for nonzero anisotropy:

$$\hbar \left(\partial_t + \vec{v}_s \cdot \vec{\nabla}\right) \vec{n} + \hbar\alpha \vec{n} \times \left(\partial_t + \frac{\beta}{\alpha} \vec{v}_s \cdot \vec{\nabla}\right) \vec{n} + \vec{n} \times \left(\vec{B} + n_z K \hat{z} + \vec{h}\right) + s^{-1} \sum_i \partial_i \vec{j}_i = 0, \tag{17}$$

where $\vec{B}$ is the magnetic field pointed in the negative z-direction, α is the Gilbert damping term [13] and $\vec{v_s}$ is the average drift velocity of the magnon cloud due to magnon-drag described in 2.2. Here, $\vec{h}$ is the field describing the steady-state stochastic fluctuations of the magnetic orientation. The final term in the above equation corresponds to the magnetic spin-current density and is given by $\vec{j}_i = -A\vec{n} \times \partial_i \vec{n}$, which is proportional to the exchange stiffness A. Assuming $B > 0$, the equilibrium orientation of our system is $\vec{n} = -\hat{z}$. Expressing the magnetic spin-current density in terms of the exchange stiffness and directional order parameter, finally yields:

$$\hbar \left(\partial_t + \vec{v}_s \cdot \vec{\nabla}\right) \vec{n} + \hbar\alpha \vec{n} \times \left(\partial_t + \frac{\beta}{\alpha} \vec{v}_s \cdot \vec{\nabla}\right) \vec{n} + \vec{n} \times \left(\vec{B} + n_z K \hat{z} + \vec{h}\right) - \frac{A}{s} \vec{n} \times \nabla^2 \vec{n} = 0. \tag{18}$$

In Fig.5, we have depicted the forces acting on the magnetization direction to illustrate the effects of the fields and interactions on the magnetization dynamics. Here we have that the effective field equals $\mathbf{H}_{eff} = B\hat{z} + n_z K \hat{z}$. Note that, contrary to [11], we have chosen the dimension of the LLG as a whole to be that of energy, rather than energy density, for convenience. This means that the dimensions of our parameters are defined as: $[s] = L^{-3}$, $[A] = JL^{-1}$ and $[B] = [K] = [\vec{h}] = J$.

3.1 Linearization

At temperatures much less than the Curie temperature, the point where materials lose their permanent magnetic properties, it suffices to linearize the magnetic dynamics with respect to

Figure 5: The magnetization, here denoted by $\mathbf{m}$, precesses about the effective field direction ($\mathbf{H_{eff}}$). The green arrow represents the dissipative (damping) torque that tends to move to magnetization to toward the effective field direction. The red arrow illustrates the spin-transfer torque while the light-blue arrow is the effective field torque with an electron spin polarization collinear with the effective field. This image was taken directly from [23].

small-angle fluctuations. In the axial configuration, this means that the magnetic field is aligned with the spin vector in the $\hat{z}$-direction, allowing us to linearize the dynamics with respect to that axis. The linearization can therefore be written as: $\vec{n} = (n_x, n_y, -1)^t$. Returning then to Eq. 16 and writing out the two cross products using the linearization, we obtain a linearized expression for the heat current:

$$\vec{\nabla}\vec{n} \times \vec{n} = \begin{vmatrix} \hat{x} & \hat{y} & \hat{z} \\ \vec{\nabla}n_x & \vec{\nabla}n_y & 0 \\ n_x & n_y & -1 \end{vmatrix} = \left(-\vec{\nabla}n_y, \vec{\nabla}n_x, 0\right)^t \tag{19}$$

and analogously we have that $\vec{n} \times \partial_t \vec{n} = (\partial_t n_y, -\partial_t n_x, 0)^t$. Therefore, the current can now be written as

$$\vec{j}_{\varepsilon,m} = -A\left(\vec{\nabla}n_y \partial_t n_y + \vec{\nabla}n_x \partial_t n_x\right). \tag{20}$$

We want to parametrize the transverse spin dynamics, so we again use the complex variables $n = n_x - in_y$ and $n^* = n_x - in_y$. Rewriting these we can express n_x and n_y in terms of these complex variables: $n_x = \frac{n+n^*}{2}$ and $n_y = \frac{n-n^*}{2i}$. Plugging into the current, we obtain:

$$\begin{aligned} \vec{j}_{\varepsilon,m} &= -A\left(\vec{\nabla}\left(\frac{n-n^*}{2i}\right)\partial_t\left(\frac{n-n^*}{2i}\right) + \vec{\nabla}\left(\frac{n+n^*}{2}\right)\partial_t\left(\frac{n+n^*}{2}\right)\right) \\ &= -\frac{A}{4}\left(-\left(\vec{\nabla}n^* - \vec{\nabla}n\right)\left(\partial_t n^* - \partial_t n\right) + \left(\vec{\nabla}n^* + \vec{\nabla}n\right)\left(\partial_t n^* + \partial_t n\right)\right) \\ &= -\frac{A}{2}\left(\vec{\nabla}n^*\partial_t n + \vec{\nabla}n\partial_t n^*\right). \end{aligned} \tag{21}$$

Since the direction of propagation in our system will be in the $\hat{x}$ direction, we Fourier transform $n(\vec{r}, t)$ and $n^*(\vec{r}, t)$ in order to express the LLG equation in terms of the magnon modes. To that end we use the following definition:

$$n(\vec{r}, t) = \int d^3q' \int d\omega' n(\vec{q}', \omega') e^{i\vec{q}'\cdot\vec{r}} e^{-i\omega' t}, \tag{22}$$

Performing the transformation:

$$\begin{aligned} j_{\varepsilon,m_x} =& \frac{A}{2}\int \frac{dk}{2\pi}\frac{d^2q}{(2\pi)^2}d\omega \frac{dk'}{2\pi}\frac{d^2q'}{(2\pi)^2}d\omega' \left(k'\omega + k\omega'\right) n(k, \vec{q}, \omega) n^*(k', \vec{q}', \omega') \\ &\times e^{i(k-k')x} e^{i(\vec{q}-\vec{q}')\cdot\vec{r}_\perp} e^{-i(\omega-\omega')t} \end{aligned} \tag{23}$$

Recalling that we are dealing with a stochastic current density, we take the average of the current. This gives us an important result:

$$\begin{aligned} \langle j_{\varepsilon,m_x} \rangle =& \frac{A}{2}\int \frac{dk}{2\pi}\frac{d^2q}{(2\pi)^2}d\omega \frac{dk'}{2\pi}\frac{d^2q'}{(2\pi)^2}d\omega' \left(k'\omega + k\omega'\right) \langle n(k, \vec{q}, \omega) n^*(k', \vec{q}', \omega') \rangle \\ &\times e^{i(k-k')x} e^{i(\vec{q}-\vec{q}')\cdot\vec{r}_\perp} e^{-i(\omega-\omega')t} \end{aligned} \tag{24}$$

In the next section, we set out to find an expression for the correlator $\langle n(k,\vec{q},\omega)n^*(k',\vec{q}',\omega')\rangle$, allowing us to evaluate Eq. 24 in section 3.2.2.

3.2 Axial configuration

In this section, we calculate the Peltier coefficient in the axial configuration. In this configuration, the anisotropy is absent, allowing us to compare our results with the magnon-drag Seebeck coefficient found in [11].

3.2.1 Correlators

Following the reasoning mentioned above, we set out to linearize the LLG and thus the magnetization dynamics. To this end we plug $\vec{n} = (n_x, n_y, -1)^t$ into our equation and work out the dot and cross products. Since n_x and n_y are small deviations from the equilibrium, we neglect terms of order $\mathcal{O}(n_i n_j)$, where $i,j \in (x,y)$. Also, since $\vec{h}$ is the stochastic fluctuation field, we neglect products of components of $\vec{n}$ and $\vec{h}$ as well. After linearizing, we arrive at the following set of equations for the three spatial components:

$$s\begin{pmatrix}\partial_t n_x + (\vec{v}_s\cdot\vec{\nabla})n_x\\ \partial_t n_y + (\vec{v}_s\cdot\vec{\nabla})n_y\\ 0\end{pmatrix} + s\alpha\begin{pmatrix}\partial_t n_y + \frac{\beta}{\alpha}(\vec{v}_s\cdot\vec{\nabla})n_y\\ -\partial_t n_x - \frac{\beta}{\alpha}(\vec{v}_s\cdot\vec{\nabla})n_x\\ 0\end{pmatrix} + \begin{pmatrix}n_y B + h_y\\ -n_x B - h_x\\ 0\end{pmatrix} + A\begin{pmatrix}-\nabla^2 n_y\\ \nabla^2 n_x\\ 0\end{pmatrix} = 0. \quad (25)$$

As we can see, the z-component of the LLG equation is zero due to only containing higher order contributions. Now we switch to the complex variables $n \equiv n_x - i n_y$ and $h \equiv h_x - i h_y$, parametrizing the transverse spin dynamics. In order to arrive at our parametrized equation, we subtract the equation for the y-component, multiplied by i, from the equation for the x-component, resulting in the following:

$$\begin{aligned} &s\left(\partial_t + (\vec{v}_s\cdot\vec{\nabla})\right)(n_x - i n_y) + s\alpha\left(\partial_t + \frac{\beta}{\alpha}(\vec{v}_s\cdot\vec{\nabla})\right)(n_y + i n_x) + B(n_y + i n_x) \quad (26)\\ &+ h_y + i h_x - A\nabla^2(n_y + i n_x) = 0. \end{aligned}$$

Using the above combined with the fact that $in = n_y + i n_x$ and multiplying through by i, we obtain:

$$is\left(\partial_t + (\vec{v}_s\cdot\vec{\nabla})\right)n(\vec{r},t) - s\alpha\left(\partial_t + \frac{\beta}{\alpha}(\vec{v}_s\cdot\vec{\nabla})\right)n(\vec{r},t) - Hn(\vec{r},t) + A\nabla^2 n(\vec{r},t) = h(\vec{r},t). \quad (27)$$

Performing a Fourier transformation with respect to time and the transverse spatial components, while setting $\vec{v}_s$ equal to zero in order to show we arrive at the same equation as in [11], we get:

$$\begin{aligned} &\int d\vec{q}' \int d\omega' \left(s\omega' + is\alpha\omega' - B + A(\partial_x^2 - q'^2)\right) n(x,\vec{q}',\omega') e^{i\vec{q}'\cdot\vec{r}_p} e^{-i\omega' t} = \quad (28)\\ &\int d\vec{q}' \int d\omega' h(x,\vec{q}',\omega') e^{i\vec{q}'\cdot\vec{r}_p} e^{-i\omega' t}. \end{aligned}$$

where $\vec{q}_\perp = \vec{q} = (q_y, q_z)$ is the transverse two-dimensional wave vector and $\vec{r}_\perp = \vec{r}_p = (y,z)$ are the transverse Cartesian coordinates. Multiplying both sides by $\int dt \int d\vec{r}_p\, e^{-i\vec{q}\cdot\vec{r}_p} e^{-i\omega t}$ allows us to construct deltas within the integral, using: $\int d\vec{r}_p\, e^{i(\vec{q}'-\vec{q})\cdot\vec{r}_p} = (2\pi)^2\delta(\vec{q}'-\vec{q})$ and

$\int dt\, e^{-i(\omega'-\omega)t} = 2\pi\delta\left(\omega'-\omega\right)$. Shown below is the result of the previously described operation.

$$\int d\vec{q}' \int d\omega' \left(s\omega' + is\alpha\omega' - B + A(\partial_x^2 - q'^2)\right) n(x,\vec{q}',\omega')\delta\left(\vec{q}'-\vec{q}\right)\delta\left(\omega'-\omega\right) = \tag{29}$$
$$\int d\vec{q}' \int d\omega' h(x,\vec{q}',\omega')\delta\left(\vec{q}'-\vec{q}\right)\delta\left(\omega'-\omega\right),$$

where the factors of 2π cancel since they appear on both sides of the equation. Working out the resulting deltas, we are left with:

$$\left(s\omega + i\alpha s\omega - B + A(\partial_x^2 - q^2)\right) n(x,\vec{q},\omega) = h(x,\vec{q},\omega) \tag{30}$$
$$A\left(\partial_x^2 - \kappa^2\right) n(x,\vec{q},\omega) = h(x,\vec{q},\omega), \tag{31}$$

where we defined $\kappa^2 \equiv q^2 + \frac{1}{A}\left(B - (1+i\alpha)s\omega\right)$. As we can see, Eq.31 indeed corresponds with the result found in [11]. Therefore, we now look at what happens when $\vec{v}_s \neq 0$. The only arising terms that differ from our $\vec{v}_s = 0$ approach are:

$$is(\vec{v}_s\cdot\vec{\nabla})n(\vec{r},t) - s\beta(\vec{v}_s\cdot\vec{\nabla})n(\vec{r},t) = 0. \tag{32}$$

Performing the same procedure as above; Fourier transforming the time and transverse spatial components, we arrive at the following equation:

$$s\left(iv_{sx}\partial_x - v_{sy}q_y - v_{sz}q_z\right)(1+i\beta)n(x,\vec{q},\omega). \tag{33}$$

Now we implement the above equation into Eq.31 in order to arrive at the transformed LLG equation relating the directional order parameter $n(x,\vec{q},\omega)$ to the steady-state stochastic fluctuations of the magnetic orientation $h(x,\vec{q},\omega)$.

$$A(\partial_x^2 + \frac{is}{A}(1+i\beta)v_{sx}\partial_x - \mu^2)n(x,\vec{q},\omega) = h(x,\vec{q},\omega), \tag{34}$$

where $\mu = q^2 + \frac{1}{A}\left(B - (1+i\alpha)s\omega + (1+i\beta)s\vec{v}_\perp\cdot\vec{q}\right)$. Here we have defined $\vec{v}_\perp = (v_{sy}, v_{sz})$ as the two-dimensional velocity vector in the transverse $\hat{y}$ and $\hat{z}$ directions. Since we have no boundaries on our fields and the temperature is constant, we can also express the x-component into momentum k using $\frac{1}{2\pi}\int dk\; n(k,\vec{q},\omega)e^{ikx}$ and multiply both sides by $\int dx\, e^{-ik'x}$, resulting in:

$$A\int dk\int dx\left(-k^2 + \frac{sv_{sx}}{A}(1+i\beta)k - \mu^2\right) n(k,\vec{q},\omega)e^{i(k-k')x} = \int dk\int dx\, h(k,\vec{q},\omega)e^{i(k-k')x}. \tag{35}$$

Working out the resulting deltas and expressing the directional order parameter in terms of the stochastic fluctuations, this expression reduces to:

$$n(k,\vec{q},\omega) = \frac{-h(k,\vec{q},\omega)}{A\left(k^2 + \frac{sv_{sx}}{A}(1+i\beta)k - \mu^2\right)}. \tag{36}$$

Now we have successfully expressed our directional order parameter in terms of the transverse magnon modes $\vec{q}$ and the propagating magnon mode k, as desired. The Langevin field stemming from the local Gilbert damping is described by the correlator [11]:

$$\langle h_i(\vec{r},\omega)h_j^*(\vec{r}',\omega')\rangle = \frac{2\pi\alpha s\hbar\omega\delta_{ij}\delta(\vec{r}-\vec{r}')\delta(\omega-\omega')}{\tanh\frac{\hbar\omega}{2k_BT}}. \tag{37}$$

Since we are ultimately interested in finding an expression for $\langle n(k,\vec{q},\omega)n^*(k',\vec{q}',\omega')\rangle$, we have to Fourier transform Eq.37 with respect to its spatial part. Since the only term depending on the spatial coordinates is $\delta(\vec{r}-\vec{r}')$, this process is straightforward. Therefore, the transformed correlator becomes

$$\langle h_i(k,\vec{q},\omega)h_j^*(k',\vec{q}',\omega')\rangle = \frac{\alpha s\hbar\omega_q\delta_{ij}\delta(k-k')\delta(\vec{q}-\vec{q}')\delta(\omega-\omega')}{(2\pi)^2\tanh\frac{\hbar\omega_q}{2k_BT}}. \tag{38}$$

Now if we multiply Eq.36 by its complex conjugate and take the average, we effectively express the correlator of the directional order parameter in terms of the correlation function of the stochastic field fluctuations.

$$\langle n_i(k,\vec{q},\omega)n_j^*(k',\vec{q}',\omega')\rangle = \frac{\langle h_i(k,\vec{q},\omega)h_j^*(k',\vec{q}',\omega')\rangle}{A^2\left|k^2+\frac{sv_{sx}}{A}(1+i\beta)k+\mu^2\right|^2}. \tag{39}$$

Straightforward plugging in of Eq.38 yields the result we are looking for

$$\langle n_i(k,\vec{q},\omega)n_j^*(k',\vec{q}',\omega')\rangle = \frac{\alpha s\hbar\omega_q\delta_{ij}\delta(k-k')\delta(\vec{q}-\vec{q}')\delta(\omega-\omega')}{(2\pi)^2A^2\left|k^2+\frac{sv_{sx}}{A}(1+i\beta)k+\mu^2\right|^2\tanh\frac{\hbar\omega_q}{2k_BT}}. \tag{40}$$

We use this expression later on to compute the charge current density corresponding to our system.

3.2.2 Evaluation of the stochastic heat current density

With the realization of an expression for the directional order parameter correlator, we return to Eq. 24 such that we are able to further compute the stochastic heat current:

$$\begin{aligned}\langle j_{\varepsilon,m_x}\rangle =& \frac{A}{2(2\pi)^6}\int dk\,d^2q\,d\omega\,dk'\,d^2q'\,d\omega'\frac{\alpha s\hbar\omega_q\left(k'\omega+k\omega'\right)\delta(k-k')\delta(\vec{q}-\vec{q}')\delta(\omega-\omega')}{(2\pi)^2A^2\left|k^2+\frac{sv_{sx}}{A}(1+i\beta)k+\mu^2\right|^2\tanh\frac{\hbar\omega_q}{2k_BT}} \\ &\times e^{i(k-k')x}e^{i(\vec{q}-\vec{q}')\cdot\vec{r}_\perp}e^{-i(\omega-\omega')t},\end{aligned} \tag{41}$$

where $\mu = q^2+\frac{1}{A}\left(B-(1+i\alpha)s\omega+(1+i\beta)s\vec{v}_\perp\cdot\vec{q}\right) = q^2+\frac{1}{A}\left(B-(1+i\alpha)s\omega\right)$ since in the $\hat{x}$-direction the $\hat{y}$ and $\hat{z}$-components of the velocity v_s are neglegible and can be set to zero. Working out the deltas, we are left with an integral over the magnon modes

$$\langle j_{\varepsilon,m_x}\rangle = \frac{\alpha s\hbar}{2(2\pi)^8A}\int dk\,d^2q\,d\omega\frac{k\omega^2}{\left|k^2+\frac{sv_{sx}}{A}(1+i\beta)k+\mu^2\right|^2\tanh\frac{\hbar\omega_q}{2k_BT}}. \tag{42}$$

In this section we will sequentially perform operations on Eq.42 in order to evaluate the four integrals present. We start by noting that α and β, the Gilbert damping parameters, are very small. However, we see that we have an α in the numerator as well as a term proportional to α^2 in the denominator. Therefore, since the integral should be valid for small damping, we take the limit $\alpha\to 0$. Furthermore, to negate the quantum fluctuations present, we let $\frac{1}{2}\coth\frac{\hbar\omega_q}{2k_BT}\to\frac{1}{2}\coth\frac{\hbar\omega_q}{2k_BT}-\frac{1}{2} = n_B(\hbar\omega_q)$, where $n_B(\hbar\omega_q)$ is the Bose-Einstein distribution accounting for the thermal fluctuations. Thus, our current now looks like:

$$\langle j_{\varepsilon,m_x}\rangle = \frac{\alpha s\hbar}{2(2\pi)^8A}\int dk\,d^2q\,d\omega\frac{k\omega^2}{\left|k^2+\frac{sv_{sx}}{A}(1+i\beta)k+\mu^2\right|^2}\left(\coth\frac{\hbar\omega_q}{2k_BT}-1\right) \tag{43}$$

First we split up the denominator into two groups of terms: one containing all damping terms and one containing the rest. Then we identify the zero points of the terms without damping, as the latter will go to zero in the low damping limit anyway. which will be useful later on. Before we do so however, let us first introduce some parameters which will simplify notation: $a \equiv \frac{sv_{sx}}{A}$, $\tilde{\omega} \equiv \frac{s\omega}{A}$ and the magnetic exchange length $\xi \equiv \sqrt{\frac{A}{B}}$. Working out gives:

$$\begin{aligned}\left|k^2 + \frac{sv_{sx}}{A}(1+i\beta)k + \mu^2\right|^2 &= \left|k^2 + \frac{sv_{sx}}{A}(1+i\beta)k + q^2 + \frac{1}{A}\left(B - (1-i\alpha)s\omega\right)\right|^2 \\ &= \left(k^2 + ak + q^2 - \tilde{\omega} + \xi^{-2}\right)^2 + \left(a\beta k - \alpha\tilde{\omega}\right)^2.\end{aligned} \tag{44}$$

Let $g(k) \equiv k^2 + ak + q^2 - \tilde{\omega} + \xi^{-2}$ and $\delta \equiv a\beta k - \alpha\tilde{\omega}$. Then the zero points follow from solving $g(k) = 0$, which results in $k_0^{\pm} = \frac{1}{2}\left(-a \pm \sqrt{a^2 - 4(q^2 - \tilde{\omega} + \xi^{-2})}\right)$. We can now write our integral as:

$$\begin{aligned}\langle j_{\varepsilon,m_x}\rangle &= \frac{A^2\hbar}{2(2\pi)^8 s^2}\int d^2q\, d\tilde{\omega}\int dk\ \tilde{\omega}^2\left(\frac{\alpha k}{g(k)^2+\delta^2}\right)\left(\coth\frac{\hbar\omega}{2k_BT} - 1\right) \\ &= \frac{A^2\hbar}{2(2\pi)^8 s^2}\int d^2q\, d\tilde{\omega}\int dk\ \frac{\alpha\tilde{\omega}^2 k}{\delta}\left(\frac{\delta}{g(k)^2+\delta^2}\right)\left(\coth\frac{\hbar\omega}{2k_BT} - 1\right).\end{aligned} \tag{45}$$

Note that in the low damping limit, $\alpha, \beta \to 0$, means that δ tends to zero as well. This is of particular interest for the first term in parenthesis, because we can approximate this term using a nascent delta function. The delta function can be viewed as the limit of a sequence of functions: $\delta = \lim_{\varepsilon\to 0}\eta_\varepsilon(x)$, where η_ε is the nascent delta function. Suppose η_ε is the Poisson kernel, which is the fundamental solution of the Laplace equation in the upper half-plane. Then we have that for:

$$\eta_\varepsilon = \frac{1}{\pi}\frac{\varepsilon}{x^2+\varepsilon^2} \qquad \Rightarrow \qquad \lim_{\varepsilon\to 0}\eta_\varepsilon = \lim_{\varepsilon\to 0}\frac{1}{\pi}\frac{\varepsilon}{x^2+\varepsilon^2} = \delta(x). \tag{46}$$

Noting that the above expression for η resembles our term in parentheses, we can write for $\eta_\alpha = \frac{\delta}{g(k)^2+\delta^2}$ in the limit that $\delta \to 0$:

$$\lim_{\delta\to 0}\eta_\alpha = \lim_{\delta\to 0}\frac{\delta}{g(k)^2+\delta^2} = \pi\delta(g(k)) = \frac{\pi\delta(k-k_0^+)}{\left|g'(k_0^+)\right|} + \frac{\pi\delta(k-k_0^-)}{\left|g'(k_0^-)\right|}, \tag{47}$$

where we made use of the identity for the composition $\delta(g(x)) = \sum_i \frac{\delta(k-k_i)}{|g(k_i)|}$, where the sum extends over all roots of $g(x)$. Consequently, using the limiting procedure described above and let $\gamma = \xi^{-2} - \tilde{\omega}$, we take the limit $\alpha, \beta \to 0$ and obtain:

$$\begin{aligned}\langle j_{\varepsilon,m_x}\rangle &= \frac{\pi A^2\hbar}{2(2\pi)^8 s^2}\int d^2q\, d\tilde{\omega}\ \alpha\tilde{\omega}^2\left(\frac{k\,\delta(k-k_0^+)}{\delta_0^+\left|g'(k_0^+)\right|} + \frac{k\,\delta(k-k_0^-)}{\delta_0^-\left|g'(k_0^-)\right|}\right)\left(\coth\frac{\hbar\omega_q}{2k_BT} - 1\right) \\ &\quad \times \Theta(a^2 > 4(q^2+\gamma))\Theta(\tilde{\omega} > -\frac{1}{4}a^2 + \xi^{-2}) \\ &= \frac{\pi A^2\hbar}{2(2\pi)^8 s^2}\int d^2q\, d\tilde{\omega}\ \alpha\tilde{\omega}^2\left(\frac{k_0^+}{\delta_0^+\left|g'(k_0^+)\right|} + \frac{k_0^-}{\delta_0^-\left|g'(k_0^-)\right|}\right)\left(\coth\frac{\hbar\omega_q}{2k_BT} - 1\right) \\ &\quad \times \Theta(a^2 > 4(q^2+\gamma))\Theta(\tilde{\omega} > -\frac{1}{4}a^2 + \xi^{-2}).\end{aligned} \tag{48}$$

Here the theta-functions arise due to the domain of validity of the low damping limit we took, outside this range the zero points would be complex. Working out the first theta-function, we get that $\Theta(a^2 > 4(q^2+\gamma)) = \Theta(q < \frac{1}{2}\sqrt{a^2-4\gamma})\Theta(q > -\frac{1}{2}\sqrt{a^2-4\gamma})$, changing the boundaries of our integral. Before we are able to apply this, we must first switch to polar coordinates to replace the double integral over $\vec{q}$ to one variable using $\int_{-\infty}^{\infty} d^2q = 2\pi \int_0^{\infty} dq\ q$. Combining the above we arrive at the following expression for the current:

$$\begin{aligned}\langle j_{\varepsilon,m_x}\rangle =& \frac{\pi A^2\hbar}{2(2\pi)^7 s^2}\int d\tilde{\omega}\Theta(\tilde{\omega} > -\frac{1}{4}a^2+\xi^{-2})\int_{-\frac{1}{2}\sqrt{a^2-4\gamma}}^{\frac{1}{2}\sqrt{a^2-4\gamma}} dq\ \alpha\tilde{\omega}^2 q\left(\coth\frac{\hbar\omega_q}{2k_BT}-1\right) \\ &\times\left(\frac{k_0^+}{\delta_0^+\left|g'(k_0^+)\right|}+\frac{k_0^-}{\delta_0^-\left|g'(k_0^-)\right|}\right).\end{aligned} \tag{49}$$

Plugging in the values of $k_0^{\pm}$ and noting that $\left|g'(k_0^+)\right| = \left|g'(k_0^-)\right| = \sqrt{a^2-4(q^2+\gamma)}$, we can simplify the last term from Eq.49 to yield:

$$\begin{aligned}\langle j_{\varepsilon,m_x}\rangle =& \frac{\pi A^2\hbar}{2(2\pi)^7 s^2}\int_{-\frac{1}{4}a^2+\xi^{-2}}^{\infty} d\tilde{\omega}\int_{-\frac{1}{2}\sqrt{a^2-4\gamma}}^{\frac{1}{2}\sqrt{a^2-4\gamma}} dq\ \frac{\alpha\tilde{\omega}^2 q}{\sqrt{a^2-4(q^2+\gamma)}}\left(\coth\frac{\hbar\omega_q}{2k_BT}-1\right) \\ &\times\frac{a\left(2\beta(q^2+\gamma)+\alpha\tilde{\omega}\right)}{a^2\left(\beta^2(q^2+\gamma)+\alpha\beta\tilde{\omega}\right)+(\alpha\tilde{\omega})^2}.\end{aligned} \tag{50}$$

Performing the integral over q using Mathematica tells us that:

$$\begin{aligned}\langle j_{\varepsilon,m_x}\rangle =& \frac{\pi\alpha A^2\hbar}{2(2\pi)^7 s^2}\int_{-\frac{1}{4}a^2+\xi^{-2}}^{\infty} d\tilde{\omega}\ \tilde{\omega}^2\left(\coth\frac{\hbar\omega_q}{2k_BT}-1\right) \\ &\times\left(\frac{\sqrt{a^2-4\gamma}}{2a\beta}-\frac{\alpha\tilde{\omega}}{a^2\beta^2}\,\mathrm{ArcSinh}\left(\frac{1}{2}a\beta\sqrt{\frac{a^2-4\gamma}{a^2\beta(\beta\gamma+\alpha\tilde{\omega})+(\alpha\tilde{\omega})^2}}\right)\right).\end{aligned} \tag{51}$$

Performing now a shift in $\tilde{\omega}$ such that the boundary does not depend on v_{sx}, i.e. on a, we use a Taylor series to approximate our current up to leading order in a. The corresponding shift should then be $\tilde{\omega} \to \tilde{\omega} + \frac{1}{4}a^2$.

$$\begin{aligned}\langle j_{\varepsilon,m_x}\rangle =& \frac{\pi\alpha A^2\hbar}{2(2\pi)^7 s^2}\int_{\xi^{-2}}^{\infty} d\tilde{\omega}\ (\tilde{\omega}+\frac{1}{4}a^2)^2\left(\coth\frac{A\hbar(\tilde{\omega}+\frac{1}{4}a^2)}{2sk_BT}-1\right) \\ &\times\left(\frac{\sqrt{2a^2-4(\xi^2-\tilde{\omega})}}{2a\beta}-\frac{\alpha\tilde{\omega}+\frac{1}{4}a^2}{a^2\beta^2}\right. \\ &\left.\times\,\mathrm{ArcSinh}\left(\frac{1}{2}a\beta\sqrt{\frac{2a^2-4(\xi^2-\tilde{\omega})}{a^2\beta(\beta(\xi^{-2}-\tilde{\omega}-\frac{1}{4}a^2)+\alpha(\tilde{\omega}+\frac{1}{4}a^2)+(\alpha(\tilde{\omega}+\frac{1}{4}a^2))^2}}\right)\right).\end{aligned} \tag{52}$$

Approximating up to linear order in a by means of a Taylor series, using Mathematica:

$$\langle j_{\varepsilon,m_x}\rangle = \frac{\pi A^2\hbar a}{2(2\pi)^7 s^2}\int_{\xi^{-2}}^{\infty} d\tilde{\omega}\ \sqrt{\tilde{\omega}-\xi^{-2}}\left(\frac{1}{2}\tilde{\omega}-\frac{\beta}{3\alpha}(\tilde{\omega}-\xi^{-2})\right)\left(\coth\frac{A\hbar\tilde{\omega}}{2sk_BT}-1\right) \tag{53}$$

Now we introduce the thermal the Broglie wavelength, in the absence of an applied field, $\lambda = \sqrt{\frac{A\hbar}{sk_BT}}$ and note that $\frac{\lambda}{\xi} = \sqrt{\frac{B\hbar}{sk_BT}}$. Of particular interest is the dimensionless variable $x = \lambda^2\tilde{\omega}$

which can be easily checked: $[x] = [\lambda^2\tilde{\omega}] = \frac{[\hbar\omega_q]}{[k_B T]} = 1$. Writing our integral in terms of x to make it dimensionless, results in

$$\langle j_{\varepsilon,m_x}\rangle = \frac{\pi A^2\hbar a}{(2\pi)^7 s^2\lambda^5}\int_{\left(\frac{\lambda}{\xi}\right)^2}^{\infty} dx\,\sqrt{x-\left(\frac{\lambda}{\xi}\right)^2}\left(\frac{1}{2}x-\frac{\beta}{3\alpha}\left(x-\left(\frac{\lambda}{\xi}\right)^2\right)\right)\left(\coth\frac{x}{2}-1\right). \quad (54)$$

We substitute x by $x' = \frac{1}{2}x$, noting that $dx' = 2dx$ and relabelling back to x, changes our integral as:

$$\langle j_{\varepsilon,m_x}\rangle = \frac{\pi A^2\hbar a}{2(2\pi)^7 s^2\lambda^5}\int_{\frac{1}{2}\left(\frac{\lambda}{\xi}\right)^2}^{\infty} dx\,\sqrt{2x-\left(\frac{\lambda}{\xi}\right)^2}\left(x-\frac{\beta}{3\alpha}\left(2x-\left(\frac{\lambda}{\xi}\right)^2\right)\right)(\coth x-1). \quad (55)$$

Now let us define $c \equiv \frac{\lambda}{\xi}$ and perform the substitution $x \to x' = \sqrt{x}$. Then we get that the new lower boundary becomes $\frac{1}{2}\left(\frac{\lambda}{\xi}\right)^2 \to \frac{1}{\sqrt{2}}\frac{\lambda}{\xi}$ and $dx = 2x'dx'$. Relabelling $x' \to x$ again, gives us:

$$\begin{aligned}\langle j_{\varepsilon,m_x}\rangle &= \frac{aA^2\hbar}{(2\pi)^6 s^2\lambda^5}\int_{\frac{c}{\sqrt{2}}}^{\infty} dx\; x\sqrt{2x^2-c^2}\left(x^2-\frac{\beta}{3\alpha}\left(2x^2-c^2\right)\right)\left(\coth x^2-1\right) \quad (56)\\ &= \frac{aA^2\hbar}{(2\pi)^6 s^2\lambda^5}\left(1-\frac{2\beta}{3\alpha}\right)\int_{\frac{c}{\sqrt{2}}}^{\infty} dx\; x\sqrt{2x^2-c^2}\left(x^2+\frac{\beta}{3\alpha-2\beta}c^2\right)\left(\coth x^2-1\right)\\ &\equiv \frac{aA^2\hbar}{(2\pi)^6 s^2\lambda^5}\left(1-\frac{2\beta}{3\alpha}\right)J[c],\end{aligned}$$

where we defined $J[c]$ as the dimensionless integral. Now since the temperature is much larger than the magnon gap, we have that $\lambda \ll \xi$. Therefore we can see that in this limit, $c \to 0$ and we calculate $J[0] = \frac{3}{16}\sqrt{\pi}\,\zeta(\frac{5}{2}) \approx 0.45$. Furthermore, we have that $a = \frac{sv_{sx}}{A}$, so in the end we are left with the following expression for our heat current density

$$\langle j_{\varepsilon,m_x}\rangle = \frac{v_{sx}}{2(2\pi)^6}\left(\frac{s}{A\hbar}\right)^{\frac{3}{2}}(k_B T)^{\frac{5}{2}}\left(1-\frac{2\beta}{3\alpha}\right)J\left[\frac{\lambda}{\xi}\right]. \quad (57)$$

We plug in that $\mathbf{v}_s = -\frac{\tilde{a}^3 P\mathbf{j}_e}{|e|}$, where P is the polarizing spin fraction of the current, $\tilde{a}$ is the lattice constant and $\mathbf{j}_e$ is the electric current density. Recall that from the linear response matrix in Eq. 2, we get that for constant temperature $\nabla T = 0$, it follows that $\mathbf{j}_e = \sigma E$. We also introduce the Curie temperature defined as $k_B T_c = A(\hbar/s)^{1/3}$. Plugging in all of the above, we arrive at:

$$\langle j_{\varepsilon,m_x}\rangle = \frac{\tilde{a}^3 Ps\sigma E k_B}{(2\pi)^6\hbar|e|}\left(\frac{\beta}{3\alpha}-\frac{1}{2}\right)\left(\frac{T}{T_c}\right)^{\frac{3}{2}}T, \quad (58)$$

from which we can finally extract the Peltier coefficient Π:

$$\Pi = \frac{\tilde{a}^3 Psk_B}{(2\pi)^6\hbar|e|}\left(\frac{\beta}{3\alpha}-\frac{1}{2}\right)\left(\frac{T}{T_c}\right)^{\frac{3}{2}}T. \quad (59)$$

Since $\tilde{a}^3 s/\hbar$ is dimensionless and $[k_B T/e] = V$ with V in units of volts, this satisfies the relation $\Pi = TS$. Here S is the Seebeck coefficient and has dimensions of volt over temperature. In order to be consistent with [11], the 1/2-term within the bracket should equal 1. Furthermore, the factor of $(2\pi)^{-6}$ should equal π^2.

3.3 Easy-plane configuration

In this section, we switch the anisotropy back on such that K is nonzero and we retrieve the easy-plane Hamiltonian defined in Eq. 5. The effective field H_{eff} corresponds to the functional derivative of $\mathcal{H}$ with respect to the directional order parameter $\vec{n}$:

$$H_{eff} = \frac{1}{s}\frac{\partial \mathcal{H}}{\partial \vec{n}} = \frac{\partial \mathcal{H}}{\partial \vec{s}} = -\frac{A}{s}\nabla^2 \vec{n} + B\hat{z} + n_z K \hat{z}. \tag{60}$$

We are interested in calculating the dispersion relation that follows from the model Hamiltonian. We want to reproduce the result found in [10], namely that for small q, where q is the wave-vector corresponding to the magnon momentum modes, the dispersion becomes linear. In this section, we calculate first the dispersion in the restricted case to verify the behaviour for small q. Then we set out to compute the full dispersion, exact in q, and use that to derive implications concerning the stability of certain regimes for $\vec{v}_s$ and damping.

3.3.1 Restricted LLG

In the case of $\alpha = \beta = \vec{v}_s = \vec{h} = 0$, we want to retrieve a linear dispersion proportional to a velocity which we will later see corresponds to the implementation of black and white hole horizons. To this end, we note that in the absence of damping and stochastic fluctuations, the LLG equation can be written as

$$\partial_t \vec{n} = \frac{1}{\hbar} H_{eff} \times \vec{n} = \left(-\frac{A}{\hbar s}\nabla^2 \vec{n} + \frac{1}{\hbar}\vec{B} + \frac{n_z}{\hbar}\vec{K} \right) \times \vec{n}. \tag{61}$$

Due to the added anisotropy in the Hamiltonian (i.e. the term proportional to K), the spin will now experience a tilt towards the xy-plane. This means that linearizing in the same way we did in section 3.2 is not possible, since the components are now coupled. Therefore we introduce the total magnon-number density $n = n_c + n_{ex}$. Here n_c represents the density of magnons occupying the lowest mode and n_{ex} corresponds to the magnon states excited above the lowest mode. In this chapter, we focus solely on magnons occupying the lowest state implying that $n_{ex} = 0$. At a finite temperature T, the thermally excited magnons also contribute to the total spin angular momentum. While assuming $T \ll T_c$, the total spin density can be written, relative to the saturated value $-s\hat{z}$ at $T = 0$, as [9]:

$$\vec{s} = (2\sqrt{s}\Re\psi, 2\sqrt{s}\Im\psi, n - s). \tag{62}$$

Here we have that $s_z = n - s = n_c - s$, since we assumed no excited magnons are present. In order to account for the tilt induced by the anisotropy we introduce the condensate order parameter $\psi = \sqrt{n_c}e^{-i\phi}$ and its complex conjugate $\psi^* = \sqrt{n_c}e^{i\phi}$, with ϕ being the xy-plane azimuthal precessional angle of the magnetization density [14].
If we now rewrite the LLG in spherical coordinates, in terms of the condensate density n_c, we get the following parametrization:

$$\vec{n} = \begin{pmatrix} \sqrt{\frac{n_c}{s}}\cos\phi \\ \sqrt{\frac{n_c}{s}}\sin\phi \\ \frac{n_c}{s} - 1 \end{pmatrix} = \begin{pmatrix} (2\sqrt{s})^{-1}(\psi + \psi^*) \\ (2i\sqrt{s})^{-1}(\psi^* - \psi) \\ \frac{|\psi|^2}{s} - 1 \end{pmatrix}. \tag{63}$$

We note that the parametrization satisfies the relation $\vec{s} = s\vec{n}$ and that the recently introduced parameters ψ and ψ^* have dimensions equal to $1/\sqrt{V}$, where V is the volume of the system.
Now that we have expressed the directional order parameter in terms of the superfluid operators,

we can recast the LLG for small-angle dynamics of the spin density around the $-\mathbf{z}$ direction. Working out the cross product in Eq.61 gives us the following equations for the x and y components; we ignore the z component as it vanishes after Fourier transforming. This is to be expected, since we can immediately see from the left-hand side that $\partial_t n_z = 0$ because n_z is constant.

$$\partial_t n_x = \left(\frac{|\psi|^2}{s} - 1\right)\left(\frac{A}{2i\hbar s\sqrt{s}}\nabla^2(\psi - \psi^*)\right) + \frac{1}{2i\hbar\sqrt{s}}\left(B + \frac{|\psi|^2}{s}K - K\right)(\psi - \psi^*), \tag{64}$$

$$\partial_t n_y = \frac{1}{2\hbar\sqrt{s}}\left(B + \frac{|\psi|^2}{s}K - K\right)(\psi + \psi^*) + \left(\frac{|\psi|^2}{s} - 1\right)\left(\frac{A}{2\hbar s\sqrt{s}}\nabla^2(\psi + \psi^*)\right). \tag{65}$$

If we look again at the parametrization in Eq.63, we note that we can write $\psi = \sqrt{s}(n_x - in_y)$ and $\psi^* = \sqrt{s}(n_x + in_y)$. Multiplying these relations by i, for convenience, we recast the two differential equations for n_x and n_y into equations for ψ and ψ^* by taking the appropriate linear combinations described above and obtain:

$$i\hbar\partial_t\psi = \frac{A}{s}\left(\frac{|\psi|^2}{s}\nabla^2\psi - \nabla^2\psi\right) - (K - B)\psi + \frac{|\psi|^2}{s}K\psi \tag{66}$$

$$i\hbar\partial_t\psi^* = -\frac{A}{s}\left(\frac{|\psi|^2}{s}\nabla^2\psi^* - \nabla^2\psi*\right) + (K - B)\psi^* - \frac{|\psi|^2}{s}K\psi^* \tag{67}$$

In the long-wavelength limit the nonlinear exchange terms vanish, which corresponds to the 1st terms of Eq.66 and 67. The long-wavelength essentially means that the wave vector is very small, i.e. $q \ll 1$, and therefore means that terms of order $\mathcal{O}(|\psi|^2\nabla^2\psi^*)$ indeed vanish after we would Fourier transform. We linearize the superfluid parameters around the condensate density by $\psi = \psi_0 + \delta\psi$ and $\psi^* = \psi_0 + \delta\psi^*$, where $\psi_0 = \sqrt{n_c}$. The absolute square then changes as: $|\psi|^2 = n_c + \psi_0(\delta\psi + \delta\psi^*)$. This ensures that our equations for ψ and ψ^* become coupled after linearization. Let $\gamma \equiv K - B$, the resulting set of coupled equations is then given by:

$$i\hbar\partial_t\psi = -\frac{A}{s}\nabla^2\delta\psi - \gamma\psi_0 - \gamma\delta\psi + \frac{1}{s}(n_c + \psi_0(\delta\psi + \delta\psi^*))K(\psi_0 + \delta\psi), \tag{68}$$

$$i\hbar\partial_t\psi^* = \frac{A}{s}\nabla^2\delta\psi^* + \gamma\psi_0 + \gamma\delta\psi^* - \frac{1}{s}(n_c + \psi_0(\delta\psi + \delta\psi^*))K(\psi_0 + \delta\psi^*). \tag{69}$$

In order to further reduce the number of dependent variables in the above equations, we set out to minimize the easy-plane Hamiltonian $\mathcal{H} = Bs_z + Ks_z^2/2s$, ignoring the exchange term, with respect to the angle θ. Plugging in $s_z = n_c - s$ gives us:

$$\begin{aligned}\mathcal{H} &= Bn_c - Bs + \frac{1}{2s}K(n_c^2 - 2n_c s + s^2) \\ &= (B - K)n_c + \frac{1}{2s}Kn_c^2 + \text{constant}.\end{aligned} \tag{70}$$

Consequently, expressing $\vec{n}$ in spherical coordinates gives the relation $n_z = -\cos\theta = n_c/s - 1$. Linearizing the cosine for small angles yields:

$$n_c = s(1 - \cos\theta) \approx s(1 - (1 - \frac{1}{2}\theta^2)) = \frac{s}{2}\theta^2. \tag{71}$$

Finally, we plug in the expression for n_c into Eq.70

$$\mathcal{H} = \frac{s}{2}(B - K)\theta^2 + \frac{s}{8}K\theta^4 + \text{constant} \tag{72}$$

and minimize with respect to θ:

$$\frac{\partial \mathcal{H}}{\partial \theta} = s(B-K)\theta + \frac{s}{2}K\theta^3 = 0 \quad \Rightarrow \quad \theta_{eq} = \pm\sqrt{\frac{2(K-B)}{K}}. \tag{73}$$

Now we have a relation for n_c in equilibrium, expressing the condensate density in terms of the saturated spin density, magnetic field and anisotropy:

$$n_{ceq} = \frac{s}{2}\theta_{eq}^2 = \frac{s(K-B)}{K} = \frac{s\gamma}{K} \tag{74}$$

We use this result to further simplify Eqs.68 and 69. We work it out in detail for the former, since it is analogous for the latter.

$$\begin{aligned} i\hbar\partial_t\psi &= -\frac{A}{s}\nabla^2\delta\psi - \gamma\psi_0 - \gamma\delta\psi + \frac{1}{s}(n_c + \psi_0(\delta\psi + \delta\psi^*))K(\psi_0 + \delta\psi) \\ &= -\frac{A}{s}\nabla^2\delta\psi - \gamma\psi_0 - \gamma\delta\psi + \gamma\psi_0 + \gamma\delta\psi + \gamma\delta\psi + \gamma\delta\psi^* + \mathcal{O}(\delta\psi^2) \\ &= -\frac{A}{s}\nabla^2\delta\psi + \gamma\delta\psi + \gamma\delta\psi^*. \end{aligned} \tag{75}$$

Therefore, simply taking the conjugate or performing the same steps as above for Eq.69, yields:

$$i\hbar\partial_t\psi^* = \frac{A}{s}\nabla^2\delta\psi^* - \gamma\delta\psi^* - \gamma\delta\psi. \tag{76}$$

In order to obtain an expression for the dispersion corresponding to our easy-plane Hamiltonian, we want to diagonalize the linearised set of equations. To this end, we will apply the Bogoliubov ansatz as described in [15] such that we are able to diagonalize the matrix. To do this, we must distinguish between negative and positive frequencies. The ansatzes are given by:

$$\delta\psi = u(\mathbf{r})e^{-i\omega t} - v^*(\mathbf{r})e^{i\omega t} \quad \text{and} \quad \delta\psi = u^*(\mathbf{r})e^{i\omega t} - v(\mathbf{r})e^{-i\omega t}. \tag{77}$$

Once again, we plug these into Eqs.75 and 76, while working it out in detail for the former:

$$\begin{aligned} &i\hbar\partial_t\psi + \frac{A}{s}\nabla^2\delta\psi - \gamma\delta\psi = -\gamma\delta\psi^* \qquad (78)\\ &(\hbar\omega_q + \frac{A}{s}\nabla^2 - \gamma)u(\mathbf{r})e^{-i\omega t} + (\hbar\omega_q - \frac{A}{s}\nabla^2 + \gamma)v^*(\mathbf{r})e^{i\omega t} = -\gamma u^*(\mathbf{r})e^{i\omega t} + \gamma v(\mathbf{r})e^{-i\omega t} \\ &((\hbar\omega_q + \frac{A}{s}\nabla^2 - \gamma)u - \gamma v)e^{-i\omega t} = ((-\hbar\omega_q + \frac{A}{s}\nabla^2 - \gamma)u^* - \gamma v^*)e^{i\omega t}. \end{aligned}$$

Straightforwardly, it follows that the conjugate equation looks like:

$$((\hbar\omega_q + \frac{A}{s}\nabla^2 - \gamma)u^* - \gamma v^*)e^{i\omega t} = ((-\hbar\omega_q + \frac{A}{s}\nabla^2 - \gamma)u - \gamma v)e^{-i\omega t}. \tag{79}$$

As can be seen from the last line of Eq.78, the equation of motion is now split up into a positive and negative frequency part. Since we want the equation to hold for any time, we conclude this can only be true if both sides are equal to zero. Therefore, if we take the left-hand side (negative frequency) to be equal to zero, we obtain the coupled set:

$$((\hbar\omega_q + \frac{A}{s}\nabla^2 - \gamma)u - \gamma v)e^{-i\omega t} = 0, \tag{80}$$

$$((-\hbar\omega_q + \frac{A}{s}\nabla^2 - \gamma)u - \gamma v)e^{-i\omega t} = 0. \tag{81}$$

We Fourier transform the fields u, v using: $u(\mathbf{r}) = u_q e^{i\mathbf{q}\cdot\mathbf{r}}$ and $v(\mathbf{r}) = v_q e^{i\mathbf{q}\cdot\mathbf{r}}$. Taking the respective derivatives, dropping the exponential terms and rewriting it in matrix form, leaves us with:

$$\begin{pmatrix} \hbar\omega_q - \frac{A}{s}q^2 - \gamma & -\gamma \\ -\gamma & -\hbar\omega_q - \frac{A}{s}q^2 - \gamma \end{pmatrix} \begin{pmatrix} u_q \\ v_q \end{pmatrix} = \begin{pmatrix} 0 \\ 0. \end{pmatrix} \tag{82}$$

The dispersion relation now follows from calculating the determinant of the matrix above. Performing this calculation yields:

$$(\hbar\omega_q)^2 = \frac{A}{s}q^2\left(\frac{A}{s}q^2 + 2\gamma\right) \quad \Rightarrow \quad \hbar\omega_q = \sqrt{\frac{A}{s}q^2\left(\frac{A}{s}q^2 + 2\gamma\right)} \tag{83}$$

Since we are, in particular, interested in the behaviour for small wave-vector, we expand the expression for small q:

$$\hbar\omega_q \approx \sqrt{\frac{2A}{s}(K-B)}q \quad \Rightarrow \quad \omega = \frac{1}{\hbar}\sqrt{\frac{2A}{s}(K-B)}q \equiv cq, \tag{84}$$

where we defined $c \equiv \frac{1}{\hbar}\sqrt{\frac{2A}{s}(K-B)}$, which has dimensions of velocity as one would expect as ω should have dimensions of frequency (i.e. t^{-1}).

3.3.2 Full LLG

Now that we have outlined our method involving superfluid parameters in the restricted case, we can move on to include the damping and stochastic terms in order to compute the dispersion and heat current corresponding to the full LLG. Therefore, less intermediate steps will be shown in this subsection, because the procedure is essentially identical and the equations are more involved than before. For this calculation, we return to Eq.17 and apply the same parametrization defined in Eq.63. The z-component is again constant and therefore vanishes upon Fourier transformation. Therefore, we look at the x and y-components instead:

$$\hbar\left(\partial_t + (\vec{v}_s\cdot\vec{\nabla})\right)n_x - \hbar\alpha n_z\left(\partial_t + \frac{\beta}{\alpha}(\vec{v}_s\cdot\vec{\nabla})\right)n_y + (B + n_z K)n_y - n_z h_y + \frac{A}{s}n_z\nabla^2 n_y = 0, \tag{85}$$

$$\hbar\left(\partial_t + (\vec{v}_s\cdot\vec{\nabla})\right)n_y + \hbar\alpha n_z\left(\partial_t + \frac{\beta}{\alpha}(\vec{v}_s\cdot\vec{\nabla})\right)n_x - (B + n_z K)n_x + n_z h_x - \frac{A}{s}n_z\nabla^2 n_x = 0, \tag{86}$$

for the x and y components respectively. We take a linear combination by subtracting Eq.86, multiplied by i, from Eq.85. That way we express the LLG in terms of the superfluid parameters ψ and ψ^*, by using Eq.63:

$$\begin{aligned} &\frac{\hbar}{\sqrt{s}}(\partial_t + (\vec{v}_s\cdot\vec{\nabla}))\psi - \alpha\frac{i\hbar}{\sqrt{s}}\left(\frac{|\psi|^2}{s} - 1\right)\left(\partial_t + \frac{\beta}{\alpha}(\vec{v}_s\cdot\vec{\nabla})\right)\psi \\ &+ \frac{i}{\sqrt{s}}\left(B + \left(\frac{|\psi|^2}{s} - 1\right)K\right)\psi - i\left(\frac{|\psi|^2}{s} - 1\right)h + i\frac{A}{s\sqrt{s}}\left(\frac{|\psi|^2}{s} - 1\right)\nabla^2\psi = 0, \end{aligned} \tag{87}$$

where we used the same relations we found for ψ in terms for n_x and n_y as in the restricted case. Multiplying through by i and bringing the stochastic term to the right hand side, gives us:

$$\begin{aligned} &\frac{i\hbar}{\sqrt{s}}(\partial_t + (\vec{v}_s\cdot\vec{\nabla}))\psi + \frac{\hbar\alpha}{\sqrt{s}}\left(\frac{|\psi|^2}{s} - 1\right)\left(\partial_t + \frac{\beta}{\alpha}(\vec{v}_s\cdot\vec{\nabla})\right)\psi \\ &- \frac{1}{\sqrt{s}}\left(B + \left(\frac{|\psi|^2}{s} - 1\right)K\right)\psi - \frac{A}{s\sqrt{s}}\left(\frac{|\psi|^2}{s} - 1\right)\nabla^2\psi = \left(1 - \frac{|\psi|^2}{s}\right)h. \end{aligned} \tag{88}$$

The first (nonlinear) term of the exchange term vanishes in the long-wavelength limit, so we will omit it from our equation again. Following the same procedure as before, we linearize the field ψ, such that we can express the equation of motion in terms of the condensate density n_c. Since we are looking at small perturbations, we also omit terms of the order $\mathcal{O}(\delta\psi^2)$ and $\mathcal{O}(\delta\psi h)$. Implementing all of the above then yields:

$$\begin{aligned}
&\left(\frac{i\hbar}{\sqrt{s}}(\partial_t + (\vec{v}_s\cdot\vec{\nabla})) - \frac{\hbar\alpha}{\sqrt{s}}\left(\partial_t + \frac{\beta}{\alpha}(\vec{v}_s\cdot\vec{\nabla})\right) + \frac{1}{\sqrt{s}}(K-B) + \frac{A}{s\sqrt{s}}\nabla^2\right)\delta\psi \\
&+ \sqrt{\frac{n_c}{s}}(K-B) + \frac{\hbar\alpha}{s\sqrt{s}}n_c\left(\partial_t + \frac{\beta}{\alpha}(\vec{v}_s\cdot\vec{\nabla})\right)\delta\psi \\
&- s^{-3/2}\left(n_cK(\psi_0+\delta\psi) + n_cK(\delta\psi+\delta\psi^*)\right) = (1-\frac{n_c}{s})h. \qquad (89)
\end{aligned}$$

Using the equilibrium relation for $n_c = s(K-B)/K$, we can simplify Eq.89 such that it reduces to:

$$\begin{aligned}
&\left(\frac{i\hbar}{\sqrt{s}}(\partial_t + (\vec{v}_s\cdot\vec{\nabla})) + \frac{\hbar\alpha}{\sqrt{s}}\left(\frac{n_c}{s}-1\right)\left(\partial_t + \frac{\beta}{\alpha}(\vec{v}_s\cdot\vec{\nabla})\right) - \frac{1}{\sqrt{s}}(K-B) + \frac{A}{s\sqrt{s}}\nabla^2\right)\delta\psi \\
&- \frac{1}{\sqrt{s}}(K-B)\delta\psi^* = \frac{B}{K}h, \qquad (90)
\end{aligned}$$

where we used that $s^{-3/2}n_c\psi_0K = \sqrt{\frac{n_c}{s}}(K-B)$ and $(1-n_c/s) = B/K$. Multiplying the entire equation by K/B and using the above, gives us:

$$\begin{aligned}
&\left(\frac{i\hbar K}{\sqrt{s}B}(\partial_t + (\vec{v}_s\cdot\vec{\nabla})) - \frac{\hbar\alpha}{\sqrt{s}}\left(\partial_t + \frac{\beta}{\alpha}(\vec{v}_s\cdot\vec{\nabla})\right) - \frac{K}{B\sqrt{s}}(K-B) + \frac{AK}{Bs\sqrt{s}}\nabla^2\right)\delta\psi \\
&- \frac{K}{B\sqrt{s}}(K-B)\delta\psi^* = h. \qquad (91)
\end{aligned}$$

Recall that we defined the magnon chemical potential as $\gamma \equiv K-B$, allowing us to rewrite Eq.91 as:

$$\left(\frac{i\hbar K}{\sqrt{s}B}(\partial_t + (\vec{v}_s\cdot\vec{\nabla})) + \frac{AK}{Bs\sqrt{s}}\nabla^2 - \frac{\hbar\alpha}{\sqrt{s}}\left(\partial_t + \frac{\beta}{\alpha}(\vec{v}_s\cdot\vec{\nabla})\right) - \frac{K}{B\sqrt{s}}\gamma\right)\delta\psi - \frac{K}{B\sqrt{s}}\gamma\delta\psi^* = h \quad (92)$$

Since Eq.92 has a conjugate counterpart, we have a set of coupled equations. To solve this, we once again perform the Bogoliubov transformation. This time, we also Fourier transform in space, such that we can immediately let all differential operators act on the exponentials. The transformations are given by:

$$\delta\psi = ue^{-i\omega t}e^{i\mathbf{q}\cdot\mathbf{r}} - v^*e^{i\omega t}e^{-i\mathbf{q}\cdot\mathbf{r}} \quad \text{and} \quad \delta\psi^* = u^*e^{i\omega t}e^{-i\mathbf{q}\cdot\mathbf{r}} - ve^{-i\omega t}e^{i\mathbf{q}\cdot\mathbf{r}}. \qquad (93)$$

The stochastic fields h and its conjugate h^* are transformed analogously to the fields in Eq.93, with fields $h_\pm$ instead of u and v (and their conjugates). Working out the derivatives while regarding only the negative frequency terms for the same reasons outlined in 3.3.1, we obtain:

$$\begin{aligned}
&\left(-\frac{\hbar K}{\sqrt{s}B}(-\omega + (\vec{v}_s\cdot\vec{q})) - \frac{AK}{Bs\sqrt{s}}q^2 - \frac{i\hbar\alpha}{\sqrt{s}}\left(-\omega + \frac{\beta}{\alpha}(\vec{v}_s\cdot\vec{q})\right) - \frac{K}{B\sqrt{s}}\gamma\right)u\,e^{-i\omega t}e^{i\mathbf{q}\cdot\mathbf{r}} \\
&+ \frac{K}{B\sqrt{s}}\gamma\,v\,e^{-i\omega t}e^{i\mathbf{q}\cdot\mathbf{r}} = h_+e^{-i\omega t}e^{i\mathbf{q}\cdot\mathbf{r}}. \qquad (94)
\end{aligned}$$

So if we then cancel the exponential terms and take the conjugate, we again arrive at a coupled set of equations for $\delta\psi$ and $\delta\psi^*$:

$$\left(-\frac{\hbar K}{\sqrt{s}B}(-\omega+(\vec{v}_s\cdot\vec{q}))-\frac{AK}{Bs\sqrt{s}}q^2-\frac{i\hbar\alpha}{\sqrt{s}}\left(-\omega+\frac{\beta}{\alpha}(\vec{v}_s\cdot\vec{q})\right)-\frac{K}{B\sqrt{s}}\gamma\right)u+\frac{K}{B\sqrt{s}}\gamma\, v=h_+, \tag{95}$$

$$\left(\frac{\hbar K}{\sqrt{s}B}(-\omega+(\vec{v}_s\cdot\vec{q}))-\frac{AK}{Bs\sqrt{s}}q^2-\frac{i\hbar\alpha}{\sqrt{s}}\left(-\omega+\frac{\beta}{\alpha}(\vec{v}_s\cdot\vec{q})\right)-\frac{K}{B\sqrt{s}}\gamma\right)v+\frac{K}{B\sqrt{s}}\gamma\, u=h_-. \tag{96}$$

For convenience, we introduce some definitions and rewrite the set of equations into matrix form: $G\equiv(-\hbar\omega_q+\hbar(\vec{v}_s\cdot\vec{q}))$, $G_d\equiv(-\hbar\omega_q+\hbar\frac{\beta}{\alpha}(\vec{v}_s\cdot\vec{q}))$, $\tilde{\gamma}=K\gamma/B\sqrt{s}$ and $J\equiv AK/B$.

$$\begin{pmatrix}-\frac{K}{B\sqrt{s}}G-\frac{J}{s\sqrt{s}}q^2-\frac{i\alpha}{\sqrt{s}}G_d-\tilde{\gamma} & \tilde{\gamma}\\ \tilde{\gamma} & \frac{K}{B\sqrt{s}}G-\frac{J}{s\sqrt{s}}q^2-\frac{i\alpha}{\sqrt{s}}G_d-\tilde{\gamma}\end{pmatrix}\begin{pmatrix}u\\ v\end{pmatrix}=\begin{pmatrix}h_+\\ h_-\end{pmatrix}. \tag{97}$$

As mentioned above, the dispersion follows from solving the homogeneous characteristic equation. So we calculate the determinant of the 2×2-matrix and equate it to zero:

$$\begin{aligned}&\left(-\frac{K}{B\sqrt{s}}G-\frac{J}{s\sqrt{s}}q^2-\frac{i\alpha}{\sqrt{s}}G_d-\tilde{\gamma}\right)\left(\frac{K}{B\sqrt{s}}G-\frac{J}{s\sqrt{s}}q^2-\frac{i\alpha}{\sqrt{s}}G_d-\tilde{\gamma}\right)-\tilde{\gamma}^2=0\\ &-\frac{K^2}{B^2s}G^2+\frac{J^2}{s^3}q^4-\frac{\alpha^2}{s}G_d^2+\tilde{\gamma}^2+2\frac{i\alpha}{s^2}JG_dq^2+2\frac{J\tilde{\gamma}}{s\sqrt{s}}q^2+2\frac{i\alpha}{\sqrt{s}}\tilde{\gamma}G_d-\tilde{\gamma}^2=0.\end{aligned} \tag{98}$$

However, since damping is generally very small, we neglect terms of second order in α and β. Plugging in the definitions for G and G_d, we get:

$$\begin{aligned}&-\frac{K^2}{B^2s}(-\hbar\omega_q+\hbar(\vec{v}_s\cdot\vec{q}))^2+\frac{J^2}{s^3}q^4+2\frac{J\tilde{\gamma}}{s\sqrt{s}}q^2+2\frac{i\alpha}{s^2}Jq^2\left(-\hbar\omega_q+\hbar\frac{\beta}{\alpha}(\vec{v}_s\cdot\vec{q})\right)\\ &+2\frac{i\alpha\tilde{\gamma}}{\sqrt{s}}\left(-\hbar\omega_q+\hbar\frac{\beta}{\alpha}(\vec{v}_s\cdot\vec{q})\right)=0.\end{aligned} \tag{99}$$

Simplifying the above equation by plugging in the definitions for J and multiplying through by B^2s/K^2:

$$\begin{aligned}&(\hbar\omega_q-\hbar(\vec{v}_s\cdot\vec{q}))^2=\frac{A^2}{s^2}q^4+2\frac{A}{s}\gamma q^2+2i\alpha\frac{BA}{Ks}q^2\left(-\hbar\omega_q+\hbar\frac{\beta}{\alpha}(\vec{v}_s\cdot\vec{q})\right)\\ &+2i\alpha\frac{B\gamma}{K}\left(-\hbar\omega_q+\hbar\frac{\beta}{\alpha}(\vec{v}_s\cdot\vec{q})\right).\end{aligned} \tag{100}$$

In Eq.100 we reverted back to our main definition of the magnon chemical potential; $\gamma=K-B$. Taking the square root and rearranging terms, we can write the equation for the dispersion as:

$$\hbar\omega_q-\hbar(\vec{v}_s\cdot\vec{q})=\sqrt{\frac{A^2}{s^2}q^4+2\frac{A}{s}\gamma q^2+2i\beta\frac{B}{K}\left(\frac{A}{s}q^2+\gamma\right)\hbar\vec{v}_s\cdot\vec{q}-2i\alpha\frac{B}{K}\left(\frac{A}{s}q^2+\gamma\right)\hbar\omega_q}. \tag{101}$$

Before we can approximate this for small damping, we have to solve for $\hbar\omega_q$ first. Solving for $\hbar\omega_q$ and expanding up to linear order in α and β yields the following expression for the dispersion:

$$\hbar\omega_q=\frac{A}{s}\sqrt{q^2(q^2+\xi^{-2})}+\hbar\vec{v}_s\cdot\vec{q}-i(\alpha-\beta)\frac{Bs\left(\frac{A}{s}q^2+\gamma\right)}{AK\sqrt{q^2(q^2+\xi^{-2})}}\hbar\vec{v}_s\cdot\vec{q}-i\alpha\frac{B}{K}\left(\frac{A}{s}q^2+\gamma\right). \tag{102}$$

Here we have defined the length scale $\xi\equiv\sqrt{\frac{A}{2s\gamma}}$, which will become useful in the next section when we make Eq. 102 dimensionless for plotting purposes.

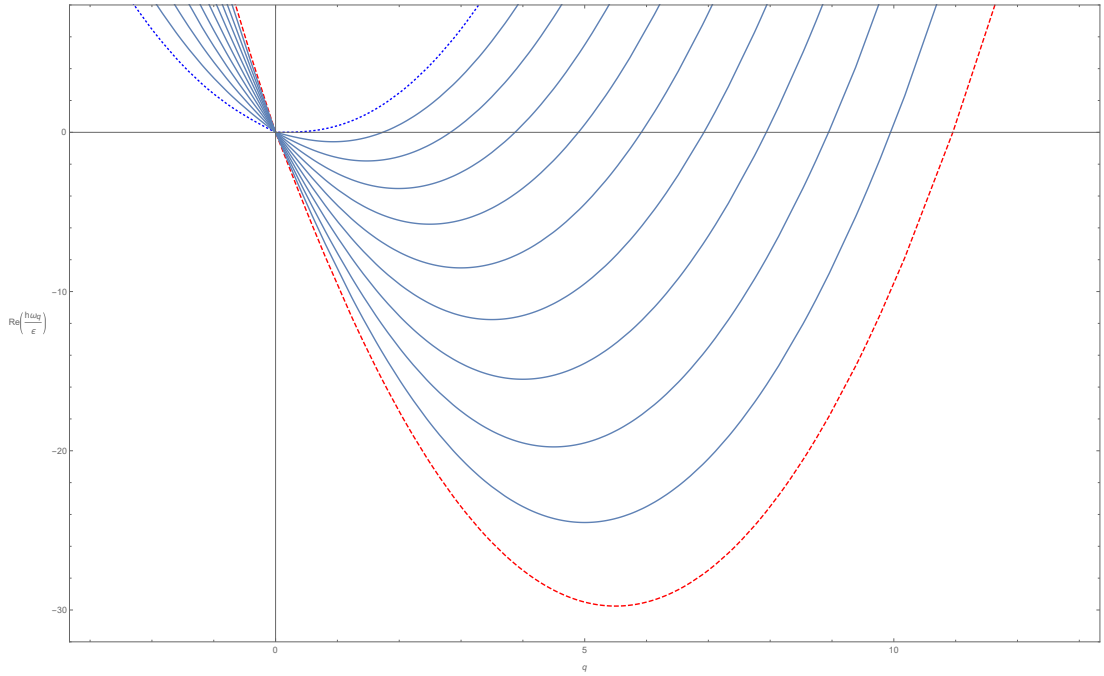

Figure 6: The real part of the dispersion plotted with respect to the (dimensionless) wave-vector $\tilde{q}$ for different values of the drift velocity $\tilde{v}$. The upper blue (dotted) line represents the threshold value $\tilde{v} = -1$ for which the dispersion does not drop below zero. This corresponds to the velocity $|\vec{v}_s| = c$ and indicates the transition from a super- to a subsonic regime or *vice versa*.

3.3.3 Dynamic instability

We devote this section to analyzing the stability of the aforementioned regions of the drift velocity $\vec{v}_s$. We do this, by looking at the real and imaginary parts of the dispersion in Eq. 102. The real part of the dispersion tells us where the threshold for $\vec{v}_s$ lies. By threshold, we mean the velocity for which the magnon cloud becomes sub- or supersonic with respect to its surrounding medium. Consequently, if we look at the imaginary part of the dispersion, we can say something about the stability of such regimes.
We start by taking the real part of Eq. 102 and make it dimensionless. To this end we recall we already introduced the length scale $\xi^2 = A/2s\gamma$ in section 3.3.2, subsequently we also define the following parameters: the energy scale $\varepsilon = A/\xi^2 s$ and the dimensionless position and velocity parameters: $\tilde{q} = q\xi$ and $\tilde{v} = \hbar\vec{v}_s/\varepsilon\xi$. This translates into:

$$\begin{aligned} \Re\hbar\omega_q &= \frac{A}{s}\sqrt{q^2(q^2+\xi^{-2})} + \hbar\vec{v}_s\cdot\vec{q} \\ \Re\frac{\hbar\omega_q}{\varepsilon} &= \sqrt{\tilde{q}^2(\tilde{q}^2+1)} + \tilde{v}\tilde{q} \end{aligned} \tag{103}$$

If we plot this for several values of $\tilde{v}$, we obtain the graph depicted in Fig. 6. We see that, for every value of $\tilde{v} < -1$, the dispersion drops below zero indicating a different regime for the magnon drift. This translates into the value of $\tilde{v} = -1$ being the threshold between the two regions. As mentioned before, these regions correspond to the super- and subsonic regimes. If

we revert back to dimensionful parameters, we see that our threshold corresponds to:

$$\tilde{v} = -1 \qquad \Rightarrow \qquad \vec{v}_s = -\frac{\varepsilon\xi}{\hbar} = -\frac{A}{s\hbar}\xi^{-1} = -\frac{1}{\hbar}\sqrt{\frac{2A}{s}(K-B)} = -c. \tag{104}$$

Therefore, as stated before, we have now proven the existence of the different regimes and verified that the threshold indeed lies at $|v_s| = c$. Thus we conclude that the magnon cloud experiences a supersonic drift for $|\vec{v}_s| > c$ and a subsonic drift for $|\vec{v}_s| < c$.
Now we wish to make some statements about the stability of said regimes. To do this, we start by taking the imaginary part of the dispersion and make it dimensionless the same way as before:

$$\Im\hbar\omega_q = -(\alpha-\beta)\frac{Bs\left(\frac{A}{s}q^2+\gamma\right)}{AK\sqrt{q^2(q^2+\xi^{-2})}}\hbar\vec{v}_s\cdot\vec{q} - \alpha\frac{B}{K}\left(\frac{A}{s}q^2+\gamma\right) \tag{105}$$

$$= -(\alpha-\beta)\frac{B\left(q^2+\frac{1}{2}\xi^{-2}\right)}{K\sqrt{q^2(q^2+\xi^{-2})}}\hbar\vec{v}_s\cdot\vec{q} - \alpha\frac{BA}{Ks}\left(q^2+\frac{1}{2}\xi^{-2}\right) \tag{106}$$

$$= (\beta-\alpha)\frac{B\left(\tilde{q}^2+\frac{1}{2}\right)}{K\sqrt{\tilde{q}^2(\tilde{q}^2+1)}}\hbar\vec{v}_s\cdot\vec{q} - \alpha\frac{BA}{Ks}\xi^{-2}\left(\tilde{q}^2+\frac{1}{2}\right), \tag{107}$$

where we rewrote the expression in terms of $\tilde{q}$. Introducing again (a different) energy scale $\varepsilon = \frac{BA}{Ks}\xi^2$ and dimensionless velocity parameter $\tilde{v} = \frac{s\hbar\vec{v}_s}{A\xi^{-1}}$, we can write:

$$\Im\frac{\hbar\omega_q}{\varepsilon} = (\beta-\alpha)\frac{\tilde{q}^2+\frac{1}{2}}{\sqrt{\tilde{q}^2(\tilde{q}^2+1)}}\tilde{v}\tilde{q} - (\tilde{q}+\frac{1}{2})\alpha. \tag{108}$$

This form allows us to plot the imaginary part for different values of $\tilde{v}$, but in this particular case, also for α and β. Therefore, we are dealing with three distinct cases for which we plot Eq. 108 for different values of $\tilde{v}$, namely $\alpha > \beta$, $\alpha = \beta$ and $\alpha < \beta$. The results can be found in the three figures below: Consider the Bogoliubov transformation in Eq. 93 and recall that

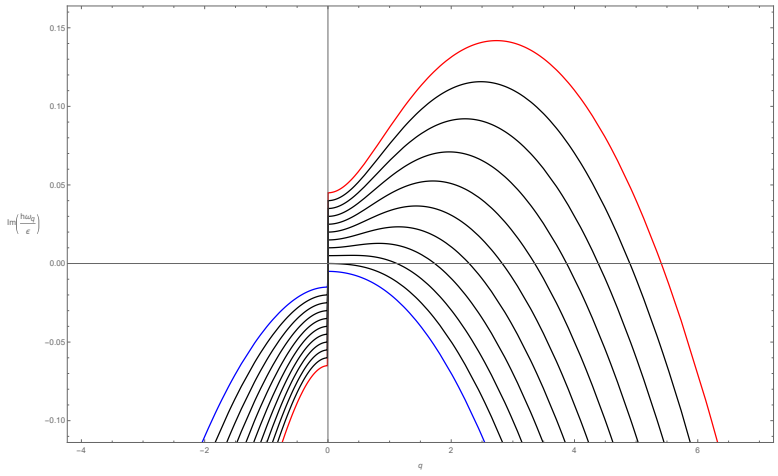

Figure 7: Here we plotted the imaginary part of the dispersion for $\alpha > \beta$. For $|\vec{v}_s| = c$, denoted by the blue line, we see that the curve does not intersect the x-axis twice. For $|\vec{v}_s| > c$ the dispersion does have two zero points, suggesting that the supersonic regime is unstable for $\alpha > \beta$.

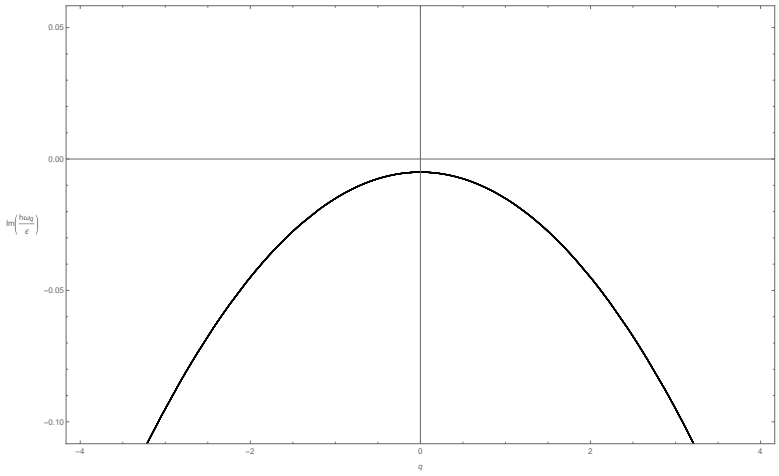

Figure 8: We see that the curve as a whole lies beneath the x-axis so for $\alpha = \beta$, both regimes are stable for all values of $\vec{v}_s$.

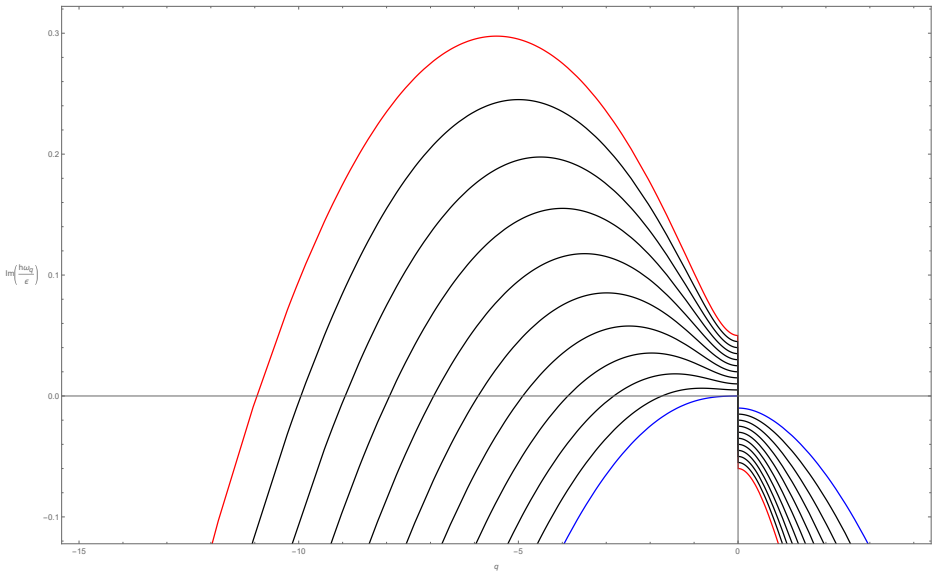

Figure 9: Here we plotted the imaginary part of the dispersion for $\alpha < \beta$. For $|\vec{v}_s| = c$, denoted by the blue line, we see that the curve does not intersect the x-axis at all. However, for $|\vec{v}_s| > 2c$ the dispersion does have two zero points, also suggesting that the supersonic regime is unstable for $\alpha < \beta$.

we chose to only regard the negative frequencies and omit the positive one. This implies that when ω actually becomes positive, the damping will not die off, therefore causing an instability. This instability occurs for positive frequencies, which corresponds to the imaginary part of the dispersion being positive. Therefore, if we look at Fig. 8, we can see that the dispersion never becomes positive implying that both regions are stable for all values of $\vec{v}_s$ and $\alpha = \beta$. However, if we glance at Fig. 7 and Fig. 9, we can see that it does contain curves above the x-axis, suggesting that these curves, which correspond to different values of $\vec{v}_s$, indicate an unstable regime. Taking a closer look at Fig. 9, reveals that the blue curve is the only one not in the upper plane. This curve corresponds to a value $\tilde{v} = -1$ or $|v_s| = c$, for $\alpha > \beta$, implying that for any curve with $|\vec{v}_s| > c$ the corresponding regime is unstable. As mentioned above, the corresponding regime in this case is the superfluid region and is therefore found to be unstable. Looking at Fig. 7 instead, we see that, for $\alpha < \beta$ the blue curve as a whole lies beneath the x-axis. It is actually the $\tilde{v} = -2$ curve that constitutes the boundary here. This implies that, in the case of $\alpha < \beta$, any system for which $|\vec{v}_s| > 2c$, the supersonic regime can be unstable. So, we have established that in the regimes for which $\alpha \neq \beta$, the supersonic regime can be unstable while the subsonic region remains stable for all values of α and β.

3.3.4 Correlators and heat current density

In order to obtain a workable expression for the stochastic heat current density, we return to Eq. 97 and invert the matrix, such that we express the Bogoliubov fields u and v in terms of the stochastic fluctuations. The second line of Eq. 98 represents the determinant of the matrix and, neglecting terms of higher than linear order in α and β, will be denoted by D in the following computations:

$$\begin{pmatrix} u \\ v \end{pmatrix} = \frac{1}{D} \begin{pmatrix} \frac{K}{B\sqrt{s}}G - \frac{J}{s\sqrt{s}}q^2 - \frac{i\alpha}{\sqrt{s}}G_d - \tilde{\gamma} & -\tilde{\gamma} \\ -\tilde{\gamma} & -\frac{K}{B\sqrt{s}}G - \frac{J}{s\sqrt{s}}q^2 - \frac{i\alpha}{\sqrt{s}}G_d - \tilde{\gamma} \end{pmatrix} \begin{pmatrix} h_+ \\ h_- \end{pmatrix}. \tag{109}$$

Suppose we write u and v as a linear combination of the form: $u = u_1 h_+ + u_2 h_-$ and $v = v_1 h_+ + v_2 h_-$. Here we defined the following parameters for convenience:

$$u_1 = \frac{-\frac{K}{B\sqrt{s}}G - \frac{J}{s\sqrt{s}}q^2 - \frac{i\alpha}{\sqrt{s}}G_d - \tilde{\gamma}}{-\frac{K^2}{B^2 s}G^2 + \frac{J^2}{s^3}q^4 + 2\frac{i\alpha}{s^2}JG_d q^2 + 2\frac{J\tilde{\gamma}}{s\sqrt{s}}q^2 + 2\frac{i\alpha}{\sqrt{s}}\tilde{\gamma}G_d} \tag{110}$$

$$v_2 = \frac{\frac{K}{B\sqrt{s}}G - \frac{J}{s\sqrt{s}}q^2 - \frac{i\alpha}{\sqrt{s}}G_d - \tilde{\gamma}}{-\frac{K^2}{B^2 s}G^2 + \frac{J^2}{s^3}q^4 + 2\frac{i\alpha}{s^2}JG_d q^2 + 2\frac{J\tilde{\gamma}}{s\sqrt{s}}q^2 + 2\frac{i\alpha}{\sqrt{s}}\tilde{\gamma}G_d} \tag{111}$$

$$u_2 = v_1 = \frac{-\tilde{\gamma}}{-\frac{K^2}{B^2 s}G^2 + \frac{J^2}{s^3}q^4 + 2\frac{i\alpha}{s^2}JG_d q^2 + 2\frac{J\tilde{\gamma}}{s\sqrt{s}}q^2 + 2\frac{i\alpha}{\sqrt{s}}\tilde{\gamma}G_d}. \tag{112}$$

Consider the expression for the stochastic heat current density as defined in Eq. 16. In order to obtain an expression in the superfluid language, we use the parametrization Eq. 63 and linearize the field ψ and its conjugate, we get:

$$\vec{j}_{\varepsilon,m} = -\frac{A}{2s}\left(\vec{\nabla}\delta\psi^* \partial_t \delta\psi + \vec{\nabla}\delta\psi \partial_t \delta\psi^*\right) \tag{113}$$

After considering only the negative frequency terms in the Bogoliubov transformation of the conjugate fields as in Eq. 93, the heat current becomes:

$$\begin{aligned}\vec{j}_{\varepsilon,m} &= -\frac{A}{2s}\int d^3q \int d^3q' \int d\omega \int d\omega' (i^2\vec{q}\omega' + i^2\vec{q}'\omega) uv\, e^{-i(\omega+\omega')t} e^{i(\vec{q}+\vec{q}')\cdot\vec{r}} \\ &= \frac{A}{2s}\int d^3q \int d^3q' \int d\omega \int d\omega' (\vec{q}\omega' + \vec{q}'\omega) uv\, e^{-i(\omega+\omega')t} e^{i(\vec{q}+\vec{q}')\cdot\vec{r}}.\end{aligned} \tag{114}$$

Noting the presence of the product uv in the expression above; we compute:

$$uv = (u_1 h_+ + u_2 h_-)(v_1 h_+ + v_2 h_-) \tag{115}$$

$$= (u_1 v_1 h_+ h_+ + u_1 v_2 h_+ h_- + u_2 v_1 h_- h_+ + u_2 v_2 h_- h_-). \tag{116}$$

We need to find a Fourier transformed expression of the correlator, such that uv can be simplified. To that end, we consider the following transformations for the fields:

$$\begin{aligned} h_+(\vec{q},\omega) &= \frac{1}{2}\int_{-\infty}^{\infty} d^3r \int_{-\infty}^{\infty} dt\, h(\vec{r},t) e^{i\omega t} e^{-i\vec{q}\cdot\vec{r}} \\ h_-(\vec{q},\omega) &= -\frac{1}{2}\int_{-\infty}^{\infty} d^3r \int_{-\infty}^{\infty} dt\, h^*(\vec{r},t) e^{i\omega t} e^{-i\vec{q}\cdot\vec{r}} \end{aligned} \tag{117}$$

This way, the transformations satisfy the Bogoliubov relation in Eq. 93. If we now Fourier transform the real space-time fields $h(\vec{r},t)$ and $h^*(\vec{r},t)$ with respect to time, i.e. $h(\vec{r},t) = \int (d\omega''/2\pi) h(\vec{r},\omega'') e^{-i\omega'' t}$ and $h^*(\vec{r},t) = \int (d\omega'''/2\pi) h^*(\vec{r},\omega''') e^{i\omega''' t}$, then we get for the product $h_+ h_-$:

$$\begin{aligned} h_+ h_- =& -\frac{1}{4}\int d^3r \int d^3r' \int dt \int dt' \int \frac{d\omega''}{2\pi} \int \frac{d\omega'''}{2\pi} h(\vec{r},\omega'') h^*(\vec{r}',\omega''') \\ & \times e^{i(\omega-\omega')t} e^{i(\omega''+\omega''')t} e^{-i\vec{q}\cdot\vec{r}} e^{-i\vec{q}'\cdot\vec{r}'} \end{aligned} \tag{118}$$

$$\begin{aligned} =& -\frac{1}{4}\int d^3r \int d^3r' \int d\omega'' \int d\omega''' h(\vec{r},\omega'') h^*(\vec{r}',\omega''') \delta(\omega-\omega'')\delta(\omega'+\omega''') \\ & \times e^{-i\vec{q}\cdot\vec{r}} e^{-i\vec{q}'\cdot\vec{r}'} \end{aligned} \tag{119}$$

$$= -\frac{1}{4}\int d^3r \int d^3r' h(\vec{r},\omega) h^*(\vec{r}',-\omega') e^{-i\vec{q}\cdot\vec{r}} e^{-i\vec{q}'\cdot\vec{r}'}. \tag{120}$$

Taking the stochastic average and plugging in the correlator from Eq. 40 with $\omega' \to -\omega'$ yields:

$$\langle h_+ h_- \rangle = -\frac{1}{4}\int d^3r \int d^3r' \langle h(\vec{r},\omega) h^*(\vec{r}',-\omega')\rangle e^{-i\vec{q}\cdot\vec{r}} e^{-i\vec{q}'\cdot\vec{r}'} \tag{121}$$

$$= -\frac{\pi\alpha s\hbar\omega}{2\tanh(\hbar\omega/2k_BT)} \int d^3\vec{r}'\, \delta(\omega+\omega') e^{-i(\vec{q}+\vec{q}')\cdot\vec{r}'}, \tag{122}$$

thus giving an expression for the correlator between $h_+(\vec{q},\omega)$ and $h_-(\vec{q}',\omega')$:

$$\langle h_+ h_- \rangle = -\frac{\pi^2\alpha s\hbar\omega\delta(\omega+\omega')\delta(\vec{q}+\vec{q}')}{\tanh(\frac{\hbar\omega}{2k_BT})}. \tag{123}$$

Note that the correlators of h_+h_+ and h_-h_- vanish and, since we are in the classical regime, $h_+h_- = h_-h_+$. This allows us to rewrite $uv = (u_1v_2 + u_2v_1)h_+h_- \equiv G_T h_+h_-$, which results in

the expression for the stochastic heat current density. Taking the stochastic average of Eq. 114:

$$\langle \vec{j}_{\varepsilon,m} \rangle = \frac{A}{2s} \int d^3q \int d^3q' \int d\omega \int d\omega' (\vec{q}\omega' + \vec{q}'\omega) \langle uv \rangle \, e^{-i(\omega+\omega')t} e^{i(\vec{q}+\vec{q}')\cdot\vec{r}} \tag{124}$$

$$= \frac{A\pi^2 \alpha s \hbar}{2s \tanh(\frac{\hbar\omega}{2k_B T})} \int d^3q \int d^3q' \int d\omega \int d\omega' (\vec{q}\omega' + \vec{q}'\omega) \omega \delta(\omega+\omega') \delta(\vec{q}+\vec{q}') G_T \tag{125}$$

$$\times \, e^{-i(\omega+\omega')t} e^{i(\vec{q}+\vec{q}')\cdot\vec{r}}.$$

Working out all the deltas, we arrive at the final expression for the heat current density:

$$\langle \vec{j}_{\varepsilon,m} \rangle = A\pi^2 \alpha \hbar \int d^3q \int d\omega \frac{\vec{q}\omega^2 G_T}{\tanh(\frac{\hbar\omega}{2k_B T})}. \tag{126}$$

Unfortunately, the evaluation of Eq. 126 can not be included here, as all time was needed for, among other things, the calculation of Eq. 59. This we leave for future readers and will be further discussed in the conclusion.

4 Conclusion

The original goal of this thesis was to find signatures for the existence of magnonic black holes in order to be able to observe, or even measure, experimentally the Hawking radiation emitted from the horizon. To this end, we considered transport experiments where we set out to calculate the magnon-drag Peltier coefficient. Before we started the calculation, we introduced some key concepts necessary for understanding the thermoelectric effects at play.

As mentioned in section 2, these concepts are governed by spin transport and its intrinsic mechanisms such as magnon-drag. The two most fundamental thermoelectric effects relevant here are the Seebeck and Peltier effects. These effects have multiple contributions stemming from both electrons and magnons. In this thesis, we focused on calculating the magnonic contribution to the Peltier effect, i.e. the magnon-drag Peltier effect. Onsager's reciprocity is a general statement about the relations between thermodynamically reversible processes. In the particular case of thermoelectric effects, it relates the Peltier and Seebeck effects by the relation $\Pi = TS$. The Seebeck effect, the reciprocal to the Peltier effect, is a conversion of heat, via an applied temperature gradient, into a build-up of voltage or electric current. The Peltier effect then is the converse effect: it translates an induced voltage into a measurable temperature gradient across the system, i.e. it transfers heat from the hot to the cold side. The Peltier effect can be viewed as the back-action counterpart to the Seebeck effect, analogous to the back-emf in magnetic induction. We subjected our ferromagnet to a charge current, which results in a partially spin-polarized current. A spin-polarized current then interacts with the magnetization dynamics through a mechanism called spin-transfer torque. Since magnons flow in the direction opposite to the spin-polarized current, they experience a drag caused by the spin-transfer torques between the magnons, or spin-waves, and electrons. This magnon-drag is essentially a Doppler shift of the spin-wave with respect to the background flow characterized by the drift velocity $\vec{v}_s$. Having clarified and explained the relevant concepts, we set out to calculate the magnon-drag Peltier coefficient.

As a starting point, we first defined the magnetic energy functional in order to compute an expression for the magnon heat current. We proceeded by defining a modified LLG equation, similar to the one in [11], which also included spin-transfer torque terms proportional to $\vec{v}_s$. Having defined our main equation governing the magnetization dynamics and the effective fields, we continued by introducing our arguments for linearization. Consequently, a linearized expression for the heat current was obtained in Eq. 16, which allowed for further evaluation. In order to be able to explicitly verify Onsager's reciprocal relation, we set the anisotropy to zero in the first calculation of the magnon-drag Peltier coefficient. In this axial configuration, the spin-vector and magnetic field were aligned, so it sufficed to linearize around the z-axis for small fluctuations in the xy-plane. The result we found was the magnon-drag Peltier coefficient in Eq. 59 and we concluded it satisfied the Onsager reciprocal relation between the Seebeck and Peltier effects, up to an independent factor of 2 in the second term. This result therefore confirmed Onsager's reciprocity in the particular case of the axial configuration. In the next section, we set $K \neq 0$ inducing a tilt from the z-axis towards the xy-plane. In this easy-plane configuration, it was no longer feasible to linearize around the z-axis, as the spin-vector and magnetic field were at a relative angle to each other. To this end, we switched to superfluid parameters, expressing the directional order parameters in terms of the condensate density n_c and superfluid fields ψ and ψ^*, allowing for coupling between the resulting equations of motion. Linearizing for small perturbations around the condensate density allowed us to effectively compute the dispersion. We calculated the dispersion both in the restricted case, i.e. no damping, drift flow and stochastic contributions, as well as in the full nonzero case. In the restricted case, we arrived at a dispersion which expanded for small wave-vector q, resulting in a linear dispersion agreeing with the

findings in [10]. In this section, we also computed the equilibrium value for n_c by minimizing the easy-plane Hamiltonian, in absence of the exchange term and stochastic contributions. This allowed us to plug in n_c after linearizing and obtain an expression for the dispersion. For the full dispersion, we followed the same procedure as in the restricted case, but kept the q dependence exact and expanded up to linear order in the damping parameters α and β.
Returning to the full dispersion, we analyzed its real and imaginary parts to obtain information about the existing regimes for the drift velocity and the corresponding stability of such regions. We plotted the real part of the dispersion, with respect to wave-vector q, for different values of $\vec{v}_s$ and found that the threshold value for which the dispersion would drop below zero, indicating a transition to another regime, to be equal to $|\vec{v}_s| = c$. For values below this threshold, the magnons propagate subsonically with respect to the background electrons, while for $|v_s| > c$ the system enters the supersonic regime. In order to say something about the stability, we consider the imaginary part, or the damping terms, of the dispersion. As it turned out, for $\beta = \alpha$, the imaginary part becomes independent of $\vec{v}_s$ and is therefore stable for all values of $\vec{v}_s$. However, for $\alpha \neq \beta$ we found that the curves lie above the x-axis for values $|\vec{v}_s| > c$, suggesting that the supersonic regime can indeed be unstable.
At this point, we were ready to calculate the stochastic heat current density for the full LLG in the easy-plane configuration. To do this, we first had to compute the expression for the heat current in terms of the superfluid parameters. Since we used the Bogoliubov transformation on the superfluid and stochastic fields, we had to modify our expression for the stochastic correlator. Once that expression had been obtained, we were able to compute the expression for the stochastic heat current density. Unfortunately, this is as far as we got during our research. We were not able to explicitly evaluate the heat current, so we were unable to see whether the temperature dependence in the magnon-drag Peltier coefficient corresponding to the easy-plane configuration differed from the axial configuration.
Summarizing, we attempted to find signatures for the existence of magnonic black hole horizons. We hypothesized that the presence of such horizons should become apparent in the expression for the magnon-drag Peltier coefficient as a different temperature dependence. Furthermore, we have outlined the phenomenology of spin transport and the key concepts surrounding the magnon-drag Peltier effect. Upon calculation of the easy-plane configuration, we realized there was not enough time to evaluate the corresponding stochastic heat current and instead made statements concerning the stability of the supersonic and subsonic regimes. We leave the evaluation of the heat current density and the eventual identification of signatures of experimental black hole horizons for magnons as an outlook for future readers and researchers. Another suggestion is to look for signatures of the supersonic instability in the heat current density or corresponding magnon-drag Peltier coefficient.

References

[1] F.Bloch. *Über die quantenmechanik der elektronen in kristallgittern.* Zeits. Phys. **52**, 555-600 (1928).

[2] H.A.Q. Enneking. *Phase diffusion in a Bose-Einstein condensate of magnons.* Institute of Theoretical Physics Utrecht, Bachelor Thesis (2015).

[3] D. Miura and A. Sakuma. *Microscopic Theory of Magnon-Drag Thermoelectric Transport in Ferromagnetic Metals.* J. Phys. Soc. Jpn., **81**, 113602 (2012).

[4] D. Avery and B.L. Zink. *Peltier Cooling and Onsager Reciprocity in Ferromagnetic Thin Films.* Phys. Rev. Lett. **111**, 126602 (2013).

[5] J. Flipse, F.K. Dejene, D. Wagenaar, G.E.W. Bauer, J. Ben Youssef and B.J. van Wees. *Observation of the Spin Peltier Effect for Magnetic Insulators.* Phys. Rev. Lett. **113**, 027601 (2014).

[6] G. N. Grannemann and L. Berger. *Magnon-drag Peltier effect in a Ni-Cu alloy.* Phys. Rev. B **13**, 2072 (1976).

[7] G.E.W. Bauer, E. Saitoh, B.J. van Wees. *Spin caloritronics.* Nature Materials **11**, 391–399 (2012).

[8] L. Onsager. *Reciprocal Relations in Irreversible Processes. I.* Phys. Rev. **37**, 405 (1931).

[9] B. Flebus, S. A. Bender, Y. Tserkovnyak and R. A. Duine. *Two-Fluid Theory for Spin Superfluidity in Magnetic Insulators.* Phys. Rev. Lett. **116**, 117201 (2016).

[10] A. Roldán-Molina, A.S. Nunez and R.A. Duine. *Magnonic Black Holes.* Phys. Rev. Lett. **118**, 061301 (2017).

[11] B. Flebus, R.A. Duine and Y. Tserkovnyak. *Landau-Lifshitz theory of the magnon-drag thermopower.* EPL (Europhysics Letters), **115**, Number 5 (2016).

[12] P.M. Haney, R.A. Duine, A.S. Núñez and A.H. MacDonald. *Current-Induced Torques in Magnetic Metals: Beyond Spin Transfer.* Journal of Magnetism and Magnetic Materials, **320**, Issue 7 1300-1311 (2008).

[13] T. Gilbert. *A Phenomenological Theory of Damping in Ferromagnetic Materials.* IEEE Transactions on Magnetics, **40**, Issue 6 3443-3449 (2004).

[14] S.A. Bender, R.A. Duine, A. Brataas and Y. Tserkovnyak. *Dynamic phase diagram of dc-pumped magnon condensates.* Phys. Rev. B **90**, 094409 (2014).

[15] C.J. Pethick, H. Smith. *Bose-Einstein Condensation in Dilute Gases.* Cambridge University Press (2002).

[16] J.Kono. *Spintronics: Coherent terahertz control.* Nature **5**, 5-6 (2011).

[17] W.G. Unruh. *Experimental Black-Hole Evaporation.* Phys. Rev. Lett. **46**, 1351 (1981).

[18] S.W. Hawking. *Black Hole Explosions.* Nature **248**, 30-31 (1974).

[19] D. C. Ralph, M.D. Stiles. *Spin Transfer Torques.* J. Magn. Magn. Mater. **320**, 1190-1216 (2008).

[20] A. Slachter, F.L. Bakker, J.P. Adam, and B.J. van Wees. *Thermally Driven Spin Injection From a Ferromagnet into a Non-magnet Metal.* Nat. Phys. **6**, pp879-882 (2010).

[21] F. K. Dejene, J. Flipse, and B.J. van Wees. *Spin-Dependent Seebeck Coefficients of Ni80Fe20 and Co in Nanopillar Spin Valves.* Phys. Rev. B, **86**, p024436 (2012).

[22] D. Qu, S.Y. Huang, J. Hu, R. Wu, and C.L. Chien. *Intrinsic Spin Seebeck Effect in Au/YIG.* Phys. Rev. Lett. **110**, p067206, (2013).

[23] A. Brataas, A.D. Kent and H. Ohno. *Current-induced torques in magnetic materials.* Nature Materials **11**, 372-381 (2012).

[24] K. Uchida, S. Takahashi, K. Harii, J. Ieda, W. Koshibae, K. Ando, S. Maekawa and E. Saitoh. *Observation of the spin-Seebeck effect.* Nature **455**, 778-781 (2008).